

Cooperativity in Chiroptical Sensing with Dendritic Zinc Porphyrins

Wei-Shi Li, Dong-Lin Jiang,* Yuki Suna, and Takuzo Aida*

Aida Nanospace Project, Exploratory Research for Advanced Technology (ERATO), Japan Science and Technology Agency (JST), 2-41 Aomi, Koto-ku, Tokyo, 135-0064 Japan

Received March 2, 2005; E-mail: jiang@nanospace.miraikan.jst.go.jp; aida@macro.t.u-tokyo.ac.jp

Dendrimers are regularly branched three-dimensional macromolecules, whose properties are dependent on the numbers of generation and branch units, along with the structures of building blocks, surface groups, and core modules.¹ Site-selective positioning of functional groups in dendritic architectures is expected to induce cooperative phenomena that may lead to a significant enhancement of certain functions. Examples of such cooperative phenomena with dendritic macromolecules have been reported for catalysis,² molecular recognition and inclusion,³ and light harvesting.⁴ We are motivated to explore the potential utility of such a cooperative phenomenon for sensory applications. Here, we report the synthesis of a series of dendritic macromolecules functionalized with multiple zinc porphyrin units (Chart 1) and highlight a clear cooperative effect on chiroptical sensing of an asymmetric ligating molecule.

Certain zinc porphyrin dimers are known to be useful for chiroptical sensing of asymmetric compounds,⁵ where the clockwise or counterclockwise-twisted geometry of the zinc porphyrin dimers is generated by ligation with chiral guests and displays an exciton-coupled circular dichroism (CD) in the visible region. Thus, we chose two- and three-branched zinc porphyrins, **2P_{Zn}** and **3P_{Zn}** (Chart 1), respectively, as the sensory parts attached to the termini of hexarylbenzene-anchored polyester dendrimers (**12P_{Zn}/24P_{Zn}** and **18P_{Zn}/36P_{Zn}**) and investigated their sensing capabilities toward **Py₂**, a chiral bidentate guest. These metalloporphyrin-appended dendrimers were unambiguously characterized by several analytical methods.^{6,7} Two-branched **2P_{Zn}**, upon titration with *RR*-**Py₂ or *SS*-**Py₂** (Chart 1) in CHCl₃, did not show any induced CD (ICD) bands at 25 °C.⁶ On the other hand, three-branched **3P_{Zn}** exhibited a certain ICD response under conditions identical to those above.⁶**

We found that **12P_{Zn}** and **24P_{Zn}**, having **2P_{Zn}** units on the dendritic scaffolds, both exhibit a strong ICD response toward the enantiomers of **Py₂**. For example, when a CHCl₃ solution of **24P_{Zn}** (0.21 μM) was titrated with *RR*-**Py₂ at 25 °C, the Soret and Q-bands of **24P_{Zn}** at 414.4 and 543.2 nm were red-shifted to 419.0 and 550.4 nm, respectively, with isosbestic points at 412.8 and 545.6 nm (Figure 1a).⁶ Thus, **24P_{Zn}** can accommodate *RR*-**Py₂, where the association constant evaluated ($K_{\text{assoc}} = 4.0 \times 10^4 \text{ M}^{-1}$; Figure 2a) is nearly 40-times as large as that of **2P_{Zn}** ($K_{\text{assoc}} = 1.0 \times 10^3 \text{ M}^{-1}$).⁶ Upon complexation with *RR*-**Py₂, **24P_{Zn}** displayed an intense positive split Cotton effect at the Soret absorption band of the zinc porphyrin units (Figure 1b, red curve). When *SS*-**Py₂** was used in place of *RR*-**Py₂**, **24P_{Zn}** exhibited a perfect mirror-image CD spectrum (blue curve) of that with *RR*-**Py₂**. The large chiroptical response of **24P_{Zn}** is originating from a twisted geometry of the guest-binding zinc porphyrin dyads on the dendrimer scaffold. In contrast, toward *RR*-**Py**, a chiral monodentate analogue of *RR*-**Py₂**, **24P_{Zn}** displayed a much lower affinity ($K_{\text{assoc}} = 4.2 \times 10^2 \text{ M}^{-1}$) and hardly showed a chiroptical response even upon addition of a large excess of *RR*-**Py** (3.4×10^5 equiv; black curve).⁶ Thus, **Py₂** actually serves as a bidentate ligand. As expected, complexation of **24P_{Zn}** with achiral *meso*-**Py₂** ($K_{\text{assoc}} = 4.0 \times 10^4 \text{ M}^{-1}$) did not result in any chiroptical response (green curve).⁶******

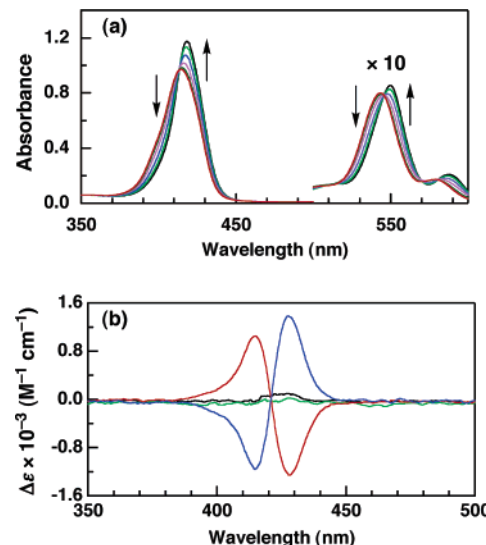


Figure 1. (a) Absorption spectral change of **24P_{Zn}** (0.21 μM) upon titration with *RR*-**Py₂ ([*RR*-**Py₂]/[**24P_{Zn}**] = 1, 6, 29, 116, 473, and 1903) in CHCl₃ at 25 °C. (b) Circular dichroism (CD) spectra of **24P_{Zn}** in the presence of *RR*-**Py₂ (red curve), *SS*-**Py₂** (blue curve), *meso*-**Py₂** (green curve) ([guest]/[**24P_{Zn}**] = 1000), and *RR*-**Py** (black curve) ([guest]/[**24P_{Zn}**] = 340 000) in CHCl₃ at 25 °C.******

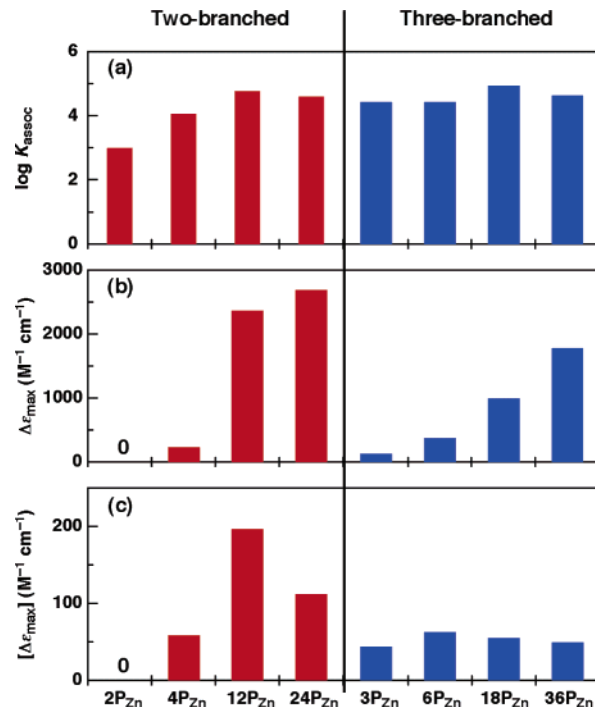
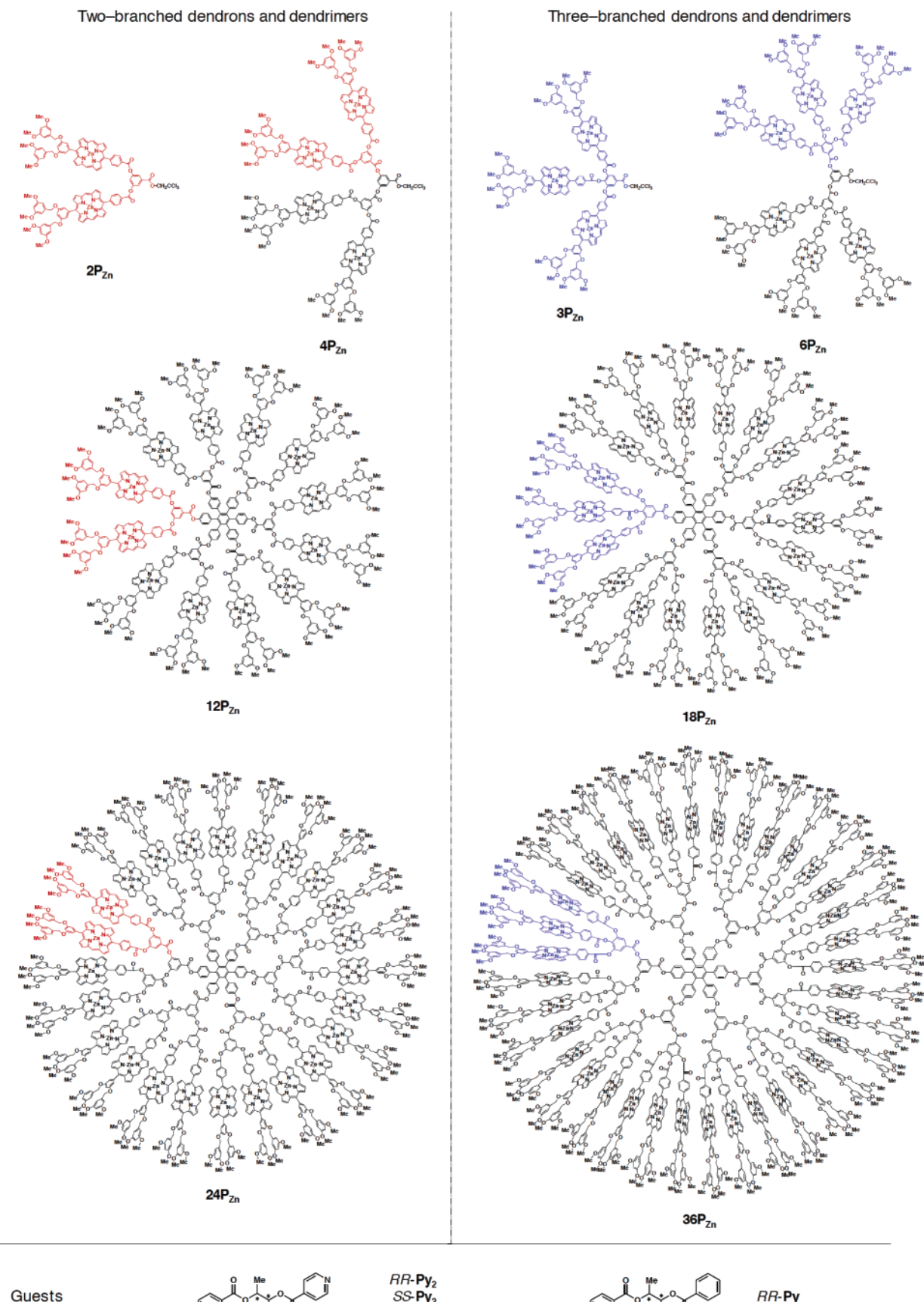


Figure 2. (a) Association constants ($\log K_{\text{assoc}}$), (b) maximum CD amplitudes ($\Delta\epsilon_{\text{max}}$), and (c) contributions of each zinc porphyrin unit to $\Delta\epsilon_{\text{max}}$ ($(\Delta\epsilon_{\text{max}})$) for dendrons **4P_{Zn}** and **6P_{Zn}**, and dendrimers **12P_{Zn}**, **18P_{Zn}**, **24P_{Zn}**, and **36P_{Zn}**, along with their precursors **2P_{Zn}** and **3P_{Zn}** in CHCl₃ at 25 °C in the presence of *RR*-**Py₂**.

Chart 1. Schematic Structures of Zinc Porphyrin-Appended Dendrons and Dendrimers Together with Guests

We also found that the capability of chiroptical sensing is highly dependent on the generation number of the dendrimer scaffold.

From a spectroscopic titration with *RR-Py*₂ in CHCl₃ at 25 °C, the K_{assoc} value of one-generation lower **12P_{Zn}** ($6.0 \times 10^4 \text{ M}^{-1}$) was

evaluated to be almost comparable to that of **24P_{Zn}** (Figure 2a). The maximum CD amplitude⁸ observed for **12P_{Zn}** ($\Delta\epsilon_{\max} = 2363 \text{ M}^{-1} \text{ cm}^{-1}$) in the presence of **RR-Py₂** was smaller than that for **24P_{Zn}** ($2693 \text{ M}^{-1} \text{ cm}^{-1}$) (Figure 2b). However, when these values were divided by the numbers of the zinc porphyrin units, one may note that the contribution of each chromophore (**P_{Zn}**) unit in **12P_{Zn}** to $\Delta\epsilon_{\max}$ ($[\Delta\epsilon_{\max}] = 196 \text{ M}^{-1} \text{ cm}^{-1}$) is much greater than that in **24P_{Zn}** ($112 \text{ M}^{-1} \text{ cm}^{-1}$) (Figure 2c). In contrast with **2P_{Zn}**, a dendron such as **4P_{Zn}** ($K_{\text{assoc}} = 1.1 \times 10^4 \text{ M}^{-1}$) exhibited a chiroptical response toward **RR-Py₂**; however, $[\Delta\epsilon_{\max}]$ was only $59 \text{ M}^{-1} \text{ cm}^{-1}$, definitely smaller than those of **12P_{Zn}** and **24P_{Zn}**. These observations indicate a possible cooperative function of the zinc porphyrin units in **12P_{Zn}** and **24P_{Zn}** for chiroptical sensing.

In sharp contrast, the zinc porphyrin units in dendrimers **18P_{Zn}** and **36P_{Zn}** did not show any cooperativity in chiral recognition, although precursor **3P_{Zn}** itself ($K_{\text{assoc}} = 2.7 \times 10^4 \text{ M}^{-1}$) exhibits a certain chiroptical response toward **Py₂**. Spectroscopic titration profiles of **18P_{Zn}** and **36P_{Zn}** with **RR-Py₂** in CHCl_3 at 25°C were virtually identical to those of **12P_{Zn}** and **24P_{Zn}**, and gave comparable K_{assoc} values of 8.9×10^4 and $4.4 \times 10^4 \text{ M}^{-1}$, respectively (Figure 2a). As shown in Figure 2b, the magnitudes of $\Delta\epsilon_{\max}$ ($\text{M}^{-1} \text{ cm}^{-1}$), upon complexation with **RR-Py₂**, are in the following order: **3P_{Zn}** (131), **18P_{Zn}** (996), and **36P_{Zn}** (1781). However, the $[\Delta\epsilon_{\max}]$ values ($\text{M}^{-1} \text{ cm}^{-1}$) of **18P_{Zn}** (55) and **36P_{Zn}** (49) are almost comparable to that of **3P_{Zn}** (43) (Figure 2c). Reference dendron **6P_{Zn}** ($K_{\text{assoc}} = 2.7 \times 10^4 \text{ M}^{-1}$) showed a $[\Delta\epsilon_{\max}]$ value of $63 \text{ M}^{-1} \text{ cm}^{-1}$, which again hardly differs from that of precursor **3P_{Zn}**.

As described in the above two sections, the K_{assoc} values of the **2P_{Zn}** series (Figure 2a, red bars) show a certain superiority of the dendrimers over the dendrons in guest binding, but the binding capabilities of dendrimers **12P_{Zn}** and **24P_{Zn}** are not much different from one another. In contrast, such a structural dependence can hardly be seen in the K_{assoc} values of the **3P_{Zn}** series (Figure 2a, blue bars). On the other hand, a more explicit difference between these two series can be seen in their chiroptical responses (Figure 2c). The $[\Delta\epsilon_{\max}]$ values of the **2P_{Zn}** series (red bars) show that **12P_{Zn}** is the better-behaved chiroptical sensor than the other, indicating the presence of an optimum structure for chiral recognition. On the other hand, the chiroptical sensing capabilities of the **3P_{Zn}** series (blue bars) hardly depend on the structure of the dendritic scaffold, and they are all much lower than that of **12P_{Zn}**. Thus, both for the guest binding and for chiroptical sensing, the zinc porphyrin units in the **2P_{Zn}** series, rather than those in the **3P_{Zn}** series, can function cooperatively.

The above trends may be related to the intramolecular interaction among the zinc porphyrin units. Thus, we conducted absorption spectroscopy in CHCl_3 at 25°C .⁶ **2P_{Zn}** showed a narrower Soret band than **3P_{Zn}** (fwhm [full width at half-maximum] = 943 and 1305 cm^{-1} , respectively), indicating a weaker ground-state interaction among the zinc porphyrin units in **2P_{Zn}**. While dendrons **4P_{Zn}**

(927 cm^{-1}) and **6P_{Zn}** (1284 cm^{-1}) were almost comparable to the corresponding precursors in terms of fwhm, the dendrimers displayed a much broader Soret band than these smaller homologues.⁶ In particular, **12P_{Zn}** and **18P_{Zn}** clearly displayed a blue-shifted shoulder in the Soret absorption region, while **24P_{Zn}** and **36P_{Zn}** only showed broadening of the Soret band without any detectable shifts (fwhm = 1558 and 2031 cm^{-1} , respectively). Of much interest, the major Soret band of **12P_{Zn}** was entirely blue-shifted by 3.8 nm from that of **2P_{Zn}**, while such a blue shift was obviously smaller for **18P_{Zn}** (1.4 nm from the Soret band of **3P_{Zn}**). From these spectral features, we assume that **12P_{Zn}** most likely possesses an efficient H-aggregated overlap of the zinc porphyrin units by a head-to-tail interaction among the neighboring **2P_{Zn}** dyads. Thanks to a smaller steric congestion of **12P_{Zn}** than the other dendrimers, such H-aggregated dyads may flexibly twist their conformation to accommodate the chiral guests, thereby displaying a large ICD response in the visible region.

Chiroptical sensing of asymmetric compounds is a subject of increasing importance for biological and medicinal applications. Here, we demonstrated a cooperative function of multiple zinc porphyrin units on the dendrimer scaffold for efficient translation of chiral information. Utilization of the resulting supramolecular chirality for asymmetric catalysis is one of the subjects worthy of further investigations.

Supporting Information Available: Details for synthesis, characterization, and spectral data (PDF). This material is available free of charge via the Internet at <http://pubs.acs.org>.

References

- (1) Fréchet, J. M. J.; Tomalia, D. A. *Dendrimers and Other Dendritic Polymers*; VCH-Wiley: New York, 2000.
- (2) (a) Riboudouille, Y.; Engel, G. D.; Richard-Plouet, M.; Gade, L. H. *Chem. Commun.* **2003**, 1228–1229. (b) Delort, E.; Darbre, T.; Reymond, J.-L. *J. Am. Chem. Soc.* **2004**, 126, 15642–15643.
- (3) (a) Zeng, F.; Zimmerman, S. C. *Chem. Rev.* **1997**, 97, 1681–1712 and references therein. (b) Epperson, J. D.; Ming, L.-J.; Baker, G. R.; Newkome, G. R. *J. Am. Chem. Soc.* **2001**, 123, 8583–8592.
- (4) (a) Jiang, D.-L.; Aida, T. *J. Am. Chem. Soc.* **1998**, 120, 10895–10901. (b) Yeow, E. K. L.; Ghiggino, K. P.; Reek, J. N. H.; Crossley, M. J.; Bosman, A. W.; Schenning, A. P. H. J.; Meijer, E. W. *J. Phys. Chem. B* **2000**, 104, 2596–2606. (c) Choi, M.-Y.; Yamazaki, T.; Yamazaki, I.; Aida, T. *Angew. Chem., Int. Ed.* **2004**, 43, 150–158.
- (5) (a) Kurtán, T.; Nesnas, N.; Li, Y.-Q.; Huang, X.; Nakanishi, K.; Berova, N. *J. Am. Chem. Soc.* **2001**, 123, 5962–5973. (b) Borovkov, V. V.; Lintuluoto, J. M.; Inoue, Y. *J. Am. Chem. Soc.* **2002**, 124, 13676–13677. (c) Mizuno, Y.; Aida, T. *Chem. Commun.* **2003**, 20–21. (d) Guo, Y.; Oike, H.; Aida, T. *J. Am. Chem. Soc.* **2004**, 126, 716–717. (e) Guo, Y.; Saeki, N.; Oike, H.; Aida, T. *Angew. Chem., Int. Ed.* **2004**, 43, 4915–4918.
- (6) See Supporting Information.
- (7) A multiporphyrin array with a hexaarylbenzene core: Lensen, M. C.; van Dingenen, S. J. T.; Elemans, J. A. A. W.; Dijkstra, H. P.; van Klink, G. P. M.; van Koten, G.; Gerritsen, J. W.; Speller, S.; Nolte, R. J. M.; Rowan, A. E. *Chem. Commun.* **2004**, 762–763.
- (8) Upon titration, the CD intensity initially increased up to a maximum value and then decreased when the guest concentration exceeded a certain point, suggesting a competition of bridging versus nonbridging ligations.

JA0513335

Supporting Information

Cooperativity in Chiroptical Sensing with Dendritic Zinc Porphyrins

Wei-Shi Li, Dong-Lin Jiang*, Yuki Suna, Takuzo Aida*

Aida Nanospace Project, Exploratory Research for Advanced Technology (ERATO), Japan Science and Technology Agency (JST), 2-41 Aomi, Koto-ku, Tokyo, 135-0064, Japan

1. Measurements and methods

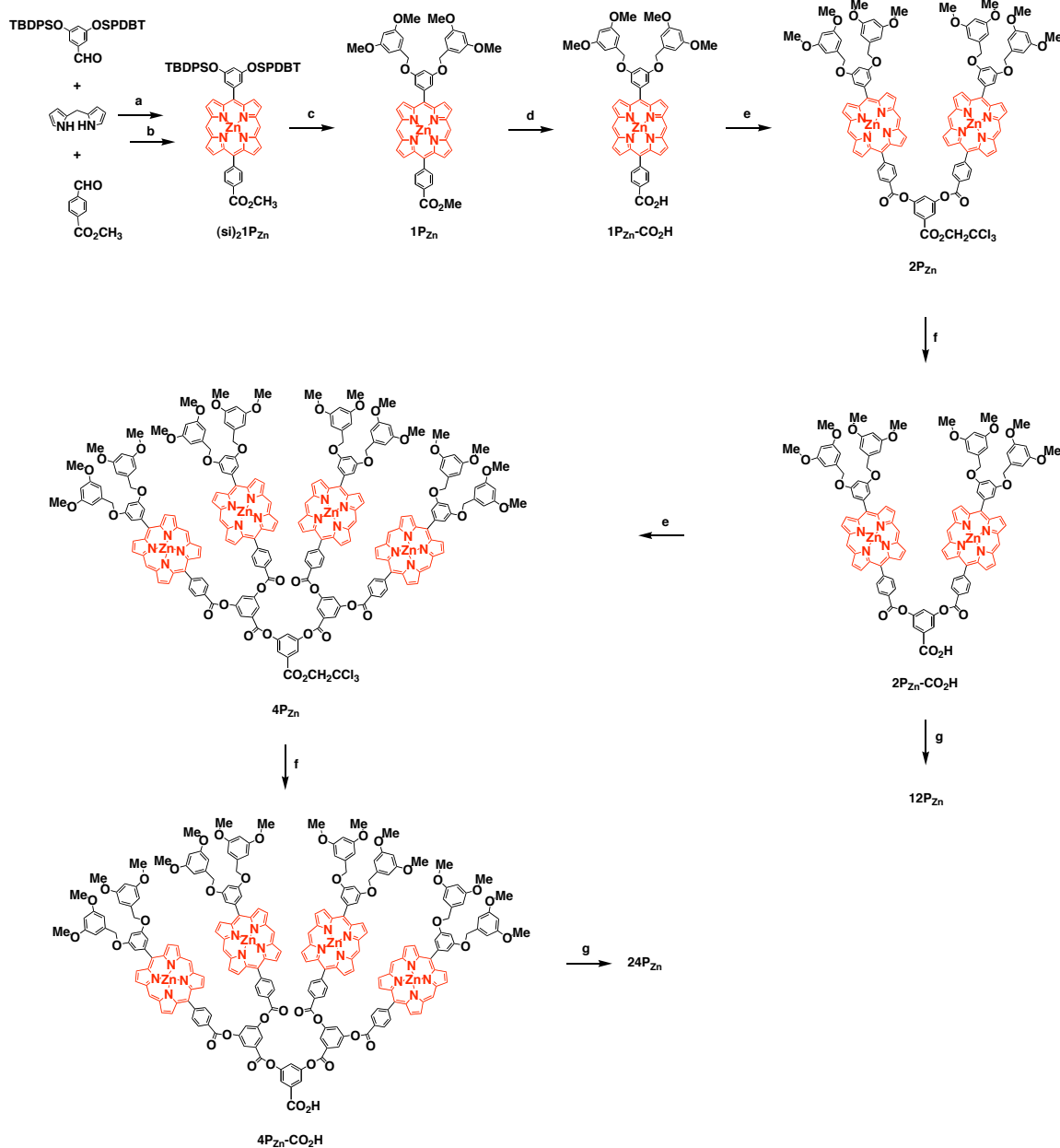
¹H NMR spectra were recorded on a JEOL model Excalibur-500 FT NMR spectrometer, where chemical shifts were determined with respect to non-deuterated solvents as internal references. MALDI-TOF-MS spectra were recorded on an Applied Biosystems model BioSpectrometry WorkstationTM Voyager-DETM STR mass spectrometer using α -cyano-4-hydroxycinnamic acid (CHCA) or dithranol as a matrix in reflector or linear mode. UV-vis and circular dichroism (CD) spectra were recorded in CHCl₃ at 25 °C using a quartz cell of 1-cm path length on a JASCO model V-570 spectrophotometer and a JASCO model J-820 spectropolarimeter, respectively. Recycling preparative SEC was performed with THF as an eluent using JAIGEL 1H (pore size: 20–30 Å), 2H (40–50 Å), and 3H (> 50 Å) columns on a JAI model LC-908 recycling HPLC system equipped with a JASCO model MD-2010 variable-wavelength UV-vis detector.

2. Materials

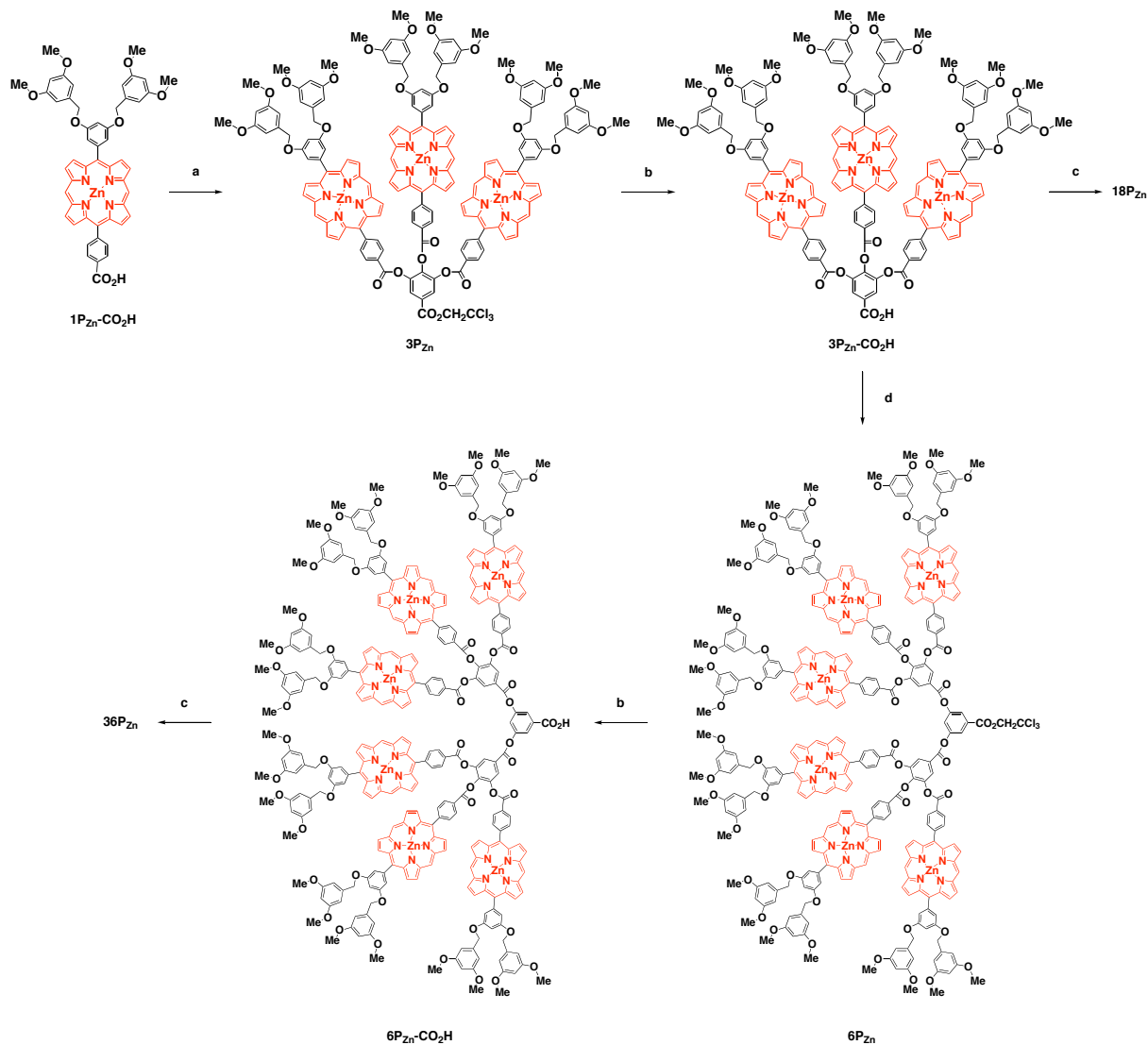
Tetrahydrofuran (THF) was distilled over sodium benzophenone ketyl under Ar (99.99%). Dehydrated-grade CH₂Cl₂ used as a reaction solvent was purchased from Wako Pure Chem. Ltd. and Kanto Chem. Ltd. 18-Crown-6 (99%), purchase from Sigma-Aldrich Fine Chemicals, was recrystallized from acetonitrile. Dicyclohexylcarbodiimide (DCC; > 95%) was purchased from Wako Pure Chem. Ltd. Anhydrous potassium fluoride (KF; 99.99%) with a water content lower than 100 ppm was purchased from Sigma-Aldrich Fine Chemicals. Dipyrromethane,¹ 3,5-di(*t*-butyldiphenylsiloxy)benzaldehyde,² 2',2',2'-trichloroethyl 3,5-dihydroxybenzoate,³ 2',2',2'-trichloroethyl 3,4,5-trihydroxybenzoate,³ hexakis(4-hydroxyphenyl)benzene,⁴ and 4-(dimethylamino)pyridium 4-toluenesulfonate (DPTS)⁵ were prepared according to literature methods.

3. Synthesis

(1) Synthesis of dendrons **2P_{Zn}**, **3P_{Zn}**, **4P_{Zn}**, and **6P_{Zn}**, and dendrimers **12P_{Zn}**, **18P_{Zn}**, **24P_{Zn}**, and **36P_{Zn}**



Scheme S1. Synthesis of **2P_{Zn}**, **4P_{Zn}**, **12P_{Zn}**, and **24P_{Zn}**. Reagents and conditions: (a) $BF_3 \cdot OEt_2$, $CH_2Cl_2/MeOH$, *p*-chloranil, r.t.; (b) $Zn(OAc)_2$, $CH_2Cl_2/MeOH$, r.t.; (c) 3,5-dimethoxy benzyl bromide, 18-crown-6, KF, THF, reflux; (d) KOH, THF/H_2O , 60 °C; (e) 2',2',2'-trichlororoethyl 3,5-dihydroxybenzoate, DCC, DPTS, CH_2Cl_2/THF , r.t.; (f) Zn powder, AcOH, THF, 60 °C; (g) hexakis(4-hydroxyphenyl)benzene, DCC, DPTS, CH_2Cl_2/THF , r.t.



Scheme S2. Synthesis of **3P_{Zn}**, **6P_{Zn}**, **18P_{Zn}**, and **36P_{Zn}**. Reagents and conditions: (a) 2',2',2'-trichloroethyl 3,4,5-trihydroxybenzoate, DCC, DPTS, CH₂Cl₂/THF, r.t.; (b) Zn powder, AcOH, THF, 60 °C; (c) hexakis(4-hydroxyphenyl)benzene, DCC, DPTS, CH₂Cl₂/THF, r.t.; (d) 2',2',2'-trichloroethyl 3,5-dihydroxybenzoate, DCC, DPTS, CH₂Cl₂/THF, r.t.

(Si)₂1P_{Zn}. A CH₂Cl₂/MeOH solution (4 L, 9/1 (v/v)) of a mixture of 3,5-di(*t*-butyldiphenylsiloxy)benzaldehyde (14.27 g, 0.023 mol), methyl 4-formylbenzoate (3.81g, 0.023mol), and dipyrromethane (6.79 g, 0.046 mol) was stirred in the presence of BF₃·OEt₂ (1.0 mL) at room temperature under Ar for 24 h in dark. To this reaction mixture was added *p*-chloranil (17 g, 0.069 mol). After 5 h, the reaction mixture was evaporated to dryness, and the residue was chromatographed on silica gel with an eluent gradually changed from CH₂Cl₂/hexane (2/1 (v/v)) to CH₂Cl₂, where the second fraction was collected and

evaporated to dryness, to give a silyl ether-protected free-base porphyrin (7 g) as purple solid in 30% yield. A CH₂Cl₂/MeOH solution (200 mL/40 mL) of a mixture of this precursor and Zn(OAc)₂·2H₂O (3 g, 0.0137 mol) was stirred overnight and evaporated to dryness. The residue was extracted with ethyl acetate, and the combined extract was dried over anhydrous Na₂SO₄, concentrated, and then chromatographed on silica gel with CH₂Cl₂ as eluent, to give (**Si**)₂**1P_{Zn}** (7.43 g) as red powder quantitatively. R_f = 0.65 (CH₂Cl₂). MS (MALDI-TOF, dithranol, reflector mode): 1092.50 ([M + H]⁺, calcd. for C₆₆H₅₈N₄O₄Si₂Zn: 1092.75). ¹H NMR (500 MHz, CDCl₃, 25 °C): δ (ppm) 10.17 (s, 2H, *meso*-H of P_{Zn}), 9.32 (d, J = 5.0 Hz, 2H, pyrrole- β -H of P_{Zn}), 9.22 (d, J = 4.0 Hz, 2H, pyrrole- β -H of P_{Zn}), 8.96 (d, J = 5.0 Hz, 2H, pyrrole- β -H of P_{Zn}), 8.64 (d, J = 4.5 Hz, 2H, pyrrole- β -H of P_{Zn}), 8.41 (d, J = 8.0 Hz, 2H, *o*-H of C₆H₄CO₂Me), 8.25 (d, J = 8.0 Hz, 2H, *m*-H of C₆H₄CO₂Me), 7.72 (m, 8H, *o*-H of SiC₆H₅), 7.43 (m, 4H, *p*-H of SiC₆H₅), 7.35 (m, 8H, *m*-H of SiC₆H₅), 7.19 (d, J = 2.0 Hz, 2H, *o*-H of P_{Zn}C₆H₃), 6.82 (t, J = 4.0 Hz, 1H, *p*-H of P_{Zn}C₆H₃), 4.10 (s, 3H, CO₂CH₃), 1.10 (s, 18H, SiC(CH₃)₃).

1P_{Zn}. A THF solution (100 mL) of a mixture of (**Si**)₂**1P_{Zn}** (3.36 g, 3.07 mmol) and 3,5-dimethoxybenzyl bromide (2.87 g, 12.4 mmol), in the presence of a mixture of 18-crown-6 (0.86 g, 3.25 mmol), K₂CO₃ (2.71 g, 19.6 mmol), and KF (3.86 g, 66.4 mmol), was refluxed under Ar for 3 days. The reaction mixture was evaporated to dryness, and the residue was extracted with CH₂Cl₂/water. The combined organic phase was concentrated and chromatographed on silica gel with CH₂Cl₂ as eluent, where the second fraction was collected and evaporated to dryness, to give **1P_{Zn}** (2.42 g) as red powder in 86% yield. R_f = 0.37 (CH₂Cl₂). MS (MALDI-TOF, dithranol, reflector mode): m/z 916.27 ([M + H]⁺). Anal. calcd. for C₅₂H₄₂N₄O₈Zn (916.30): C 68.2, H 4.6, N 6.1, Zn 7.1; found C 67.9, H 4.8, N 5.6, Zn 6.7. ¹H NMR (500 MHz, CDCl₃, 25 °C): δ (ppm) 10.29 (s, 2H, *meso*-H of P_{Zn}), 9.41 (d, J = 4.5 Hz, 2H, pyrrole- β -H of P_{Zn}), 9.39 (d, J = 4.5 Hz, 2H, pyrrole- β -H of P_{Zn}), 9.17 (d, J = 4.0 Hz, 2H, pyrrole- β -H of P_{Zn}), 9.04 (d, J = 5.0 Hz, 2H, pyrrole- β -H of P_{Zn}), 8.42 (d, J = 3.5 Hz, 2H, *o*-H of C₆H₄CO₂Me), 8.31 (d, J = 3.0 Hz, 2H, *m*-H of C₆H₄CO₂Me), 7.51 (d, J = 2.5 Hz, 2H, *o*-H of P_{Zn}C₆H₃), 7.04 (t, J = 4.0 Hz, 1H, *p*-H of P_{Zn}C₆H₃), 6.62 (d, J = 2.0 Hz, 4H, *o*-H of outer C₆H₃), 6.40 (t, J = 4.5 Hz, 2H, *p*-H of outer C₆H₃), 5.15 (s, 4H, ArCH₂OAr), 4.08 (s, 3H, CO₂CH₃), 3.75 (s, 12H, ArOCH₃). UV-Vis (CHCl₃, 25 °C): 413.4, 540.8, 575.2 nm.

1P_{Zn}-CO₂H. To a THF solution (10 mL) of **1P_{Zn}** (0.26 g, 0.284 mmol) was added an aqueous KOH solution (5 mL, 0.34 M), and the mixture was stirred at 60 °C for 12 h under Ar.

The reaction mixture was neutralized with acetic acid and extracted with ethyl acetate. The combined organic phase was washed with water, evaporated to dryness, and the residue was reprecipitated from THF/hexane, to give **1P_{Zn}-CO₂H** (0.24 g) as red powder in 95% yield. MS (MALDI-TOF, dithranol, reflector mode): m/z 900.57 ([M - H]⁺, calcd. for C₅₁H₄₀N₄O₈Zn: 902.28). ¹H NMR (500 MHz, acetone-d₆, 25 °C): δ (ppm) 11.47 (b, 1H, COOH), 10.36 (s, 2H, *meso*-H of P_{Zn}), 9.47–9.03 (m, 8H, pyrrole-β-H of P_{Zn}), 8.49 (d, *J* = 8.0 Hz, 2H, *o*-H of C₆H₄CO₂H), 8.37 (d, *J* = 8.0 Hz, 2H, *m*-H of C₆H₄CO₂H), 7.94 (b, 2H, *o*-H of P_{Zn}C₆H₃), 7.14 (s, 1H, *p*-H of P_{Zn}C₆H₃), 6.72 (s, 4H, *o*-H of outer C₆H₃), 6.46 (s, 2H, *p*-H of outer C₆H₃), 5.29 (s, 4H, ArCH₂OAr), 3.77 (s, 12H, ArOCH₃).

2P_{Zn}. To a THF solution (5 mL) of a mixture of **1P_{Zn}-CO₂H** (0.45 g, 0.5 mmol) and 2',2',2'-trichloroethyl 3,5-dihydroxybenzoate (58 mg, 0.2 mmol) was slowly added under Ar a CH₂Cl₂ solution (5 mL) of DPTS (73.0 mg, 0.248 mmol). After 10 min, a CH₂Cl₂ solution (5 mL) of DCC (154 mg, 0.746 mmol) was added to the above solution, and the mixture was stirred for 2 days at room temperature. The insoluble fraction formed was filtered off, and the filtrate was concentrated and chromatographed on silica gel with CH₂Cl₂/THF (100/5 (v/v)) as an eluent, where the first fraction was evaporated to dryness and subjected to recycling preparative SEC (1H/2H columns) with THF as an eluent, to allow isolation of **2P_{Zn}** (0.39 g) as red powder in 95% yield. *R_f* = 0.59 (CH₂Cl₂/THF = 100/5 (v/v)). MS (MALDI-TOF, dithranol, reflector mode): m/z 2053.26 ([M + H]⁺). Anal. calcd. for C₁₁₁H₈₃Cl₃N₈O₁₈Zn₂ (2054.03): C 64.9, H 4.1, N 5.5, Cl 5.2, Zn 6.4; found C 63.3, H 4.5, N 4.8, Cl 5.6, Zn 5.7. ¹H NMR (500 MHz, CDCl₃, 25 °C): δ (ppm) 10.28 (s, 4H, *meso*-H of P_{Zn}), 9.44–9.08 (m, 16H, pyrrole-β-H of P_{Zn}), 8.57 (d, *J* = 9.0 Hz, 4H, *o*-H of P_{Zn}C₆H₄CO₂Ar), 8.42 (d, *J* = 7.5 Hz, 4H, *m*-H of P_{Zn}C₆H₄CO₂Ar), 8.00 (d, *J* = 2.5 Hz, 2H, *o*-H of C₆H₃CO₂CH₂CCl₃), 7.64 (t, *J* = 2.0 Hz, 1H, *p*-H of C₆H₃CO₂CH₂CCl₃), 7.52 (d, *J* = 2.0 Hz, 4H, *o*-H of P_{Zn}C₆H₃), 7.04 (t, *J* = 4.0 Hz, 2H, *p*-H of P_{Zn}C₆H₃), 6.58 (d, *J* = 2.5 Hz, 8H, *o*-H of outer C₆H₃), 6.36 (t, *J* = 4.0 Hz, 4H, *p*-H of outer C₆H₃), 5.13 (s, 8H, ArCH₂OAr), 5.00 (s, 2H, CO₂CH₂CCl₃), 3.72 (s, 24H, ArOCH₃). UV-vis (CHCl₃, 25 °C): 414.8, 541.8, 576.6 nm.

2P_{Zn}-CO₂H. A THF/AcOH solution (5 mL/5 mL) of a mixture of **2P_{Zn}** (0.39 g, 0.19 mmol) and zinc powder (0.26 mg, 3.92 mmol) was stirred at 60 °C for 6 h. The insoluble fraction was filtered off, and the filtrate was concentrated and chromatographed on silica gel with CH₂Cl₂/THF (100/5 (v/v)) as an eluent, where the first fraction was evaporated, and the residue was reprecipitated from THF/hexane, to give **2P_{Zn}-CO₂H** (0.31 g) as red powder in

86% yield. $R_f = 0.30$ ($\text{CH}_2\text{Cl}_2/\text{THF} = 100/5$ (v/v)). MS (MALDI-TOF, dithranol, reflector mode): m/z 1920.26 ($[\text{M} - \text{H}]^+$, calcd. for $\text{C}_{109}\text{H}_{82}\text{N}_8\text{O}_{18}\text{Zn}_2$: 1922.64). ^1H NMR (500 MHz, CDCl_3 , 25 °C): δ (ppm) 10.17 (s, 4H, *meso*-H of P_{Zn}), 9.35–9.06 (m, 16H, pyrrole- β -H of P_{Zn}), 8.60 (d, $J = 7.0$ Hz, 4H, *o*-H of $\text{P}_{\text{Zn}}\text{C}_6\text{H}_4\text{CO}_2\text{Ar}$), 8.42 (d, $J = 7.0$ Hz, 4H, *m*-H of $\text{P}_{\text{Zn}}\text{C}_6\text{H}_4\text{CO}_2\text{Ar}$), 8.08 (b, 2H, *o*-H of $\text{C}_6\text{H}_3\text{CO}_2\text{H}$), 7.74 (b, 1H, *p*-H of $\text{C}_6\text{H}_3\text{CO}_2\text{H}$), 7.52 (s, 4H, *o*-H of $\text{P}_{\text{Zn}}\text{C}_6\text{H}_3$), 7.02 (s, 2H, *p*-H of $\text{P}_{\text{Zn}}\text{C}_6\text{H}_3$), 6.58 (s, 8H, *o*-H of outer C_6H_3), 6.36 (s, 4H, *p*-H of outer C_6H_3), 5.12 (s, 8H, ArCH_2OAr), 3.71 (s, 24H, ArOCH_3).

4P_{Zn}. To a THF solution (2 mL) of a mixture of **2P_{Zn}-CO₂H** (0.25 g, 0.13 mmol) and 2',2',2'-trichloroethyl 3,5-dihydroxybenzoate (16.8 mg, 0.06 mmol) was slowly added under Ar a CH_2Cl_2 solution (4 mL) of DPTS (22.4 mg, 0.076 mmol). After 10 min, a CH_2Cl_2 solution (4 mL) of DCC (46.3 mg, 0.224 mmol) was added to the above solution, and the reaction mixture was stirred for 3 days at room temperature. The reaction mixture was treated in a manner similar to that described for **2P_{Zn}**, to give **4P_{Zn}** (0.26 g) as red powder in 94% yield. $R_f = 0.70$ ($\text{CH}_2\text{Cl}_2/\text{THF} = 100/5$ (v/v)). MS (MALDI-TOF, dithranol, reflector mode): m/z 4094.37 ($[\text{M} + \text{H}]^+$, calcd. for $\text{C}_{227}\text{H}_{167}\text{Cl}_3\text{N}_{16}\text{O}_{38}\text{Zn}_4$: 4094.76). ^1H NMR (500 MHz, $\text{THF}-d_8$, 25 °C): δ (ppm) 10.26 (s, 8H, *meso*-H of P_{Zn}), 9.44–9.07 (m, 32H, pyrrole- β -H of P_{Zn}), 8.76 (d, $J = 7.5$ Hz, 8H, *o*-H of $\text{P}_{\text{Zn}}\text{C}_6\text{H}_4\text{CO}_2\text{Ar}$), 8.51 (d, $J = 7.5$ Hz, 8H, *m*-H of $\text{P}_{\text{Zn}}\text{C}_6\text{H}_4\text{CO}_2\text{Ar}$), 8.45 (d, $J = 1.5$ Hz, 4H, *o*-H of $\text{C}_6\text{H}_3\text{CO}_2\text{Ar}$), 8.25 (t, $J = 2.0$ Hz, 2H, *p*-H of $\text{C}_6\text{H}_3\text{CO}_2\text{Ar}$), 8.11 (d, $J = 4.5$ Hz, 2H, *o*-H of $\text{C}_6\text{H}_3\text{CO}_2\text{CH}_2\text{CCl}_3$), 8.04 (t, $J = 5.0$ Hz, 1H, *p*-H of $\text{C}_6\text{H}_3\text{CO}_2\text{CH}_2\text{CCl}_3$), 7.53 (d, $J = 2.0$ Hz, 8H, *o*-H of $\text{P}_{\text{Zn}}\text{C}_6\text{H}_3$), 7.14 (t, $J = 4.5$ Hz, 4H, *p*-H of $\text{P}_{\text{Zn}}\text{C}_6\text{H}_3$), 6.67 (d, $J = 2.0$ Hz, 16H, *o*-H of outer C_6H_3), 6.42 (t, 8H, $J = 5.0$ Hz, *p*-H of outer C_6H_3), 5.20 (s, 18H, ArCH_2OAr and $\text{CO}_2\text{CH}_2\text{CCl}_3$), 3.70 (s, 48H, ArOCH_3). UV-vis (CHCl_3 , 25 °C): 414.8, 542.0, 576.6 nm.

4P_{Zn}-CO₂H. A THF/AcOH solution (5 mL/5 mL) of a mixture of **4P_{Zn}** (0.22 g, 0.055 mmol) and zinc powder (0.52 mg, 9.34 mmol) was stirred for 6 h at 60 °C. The reaction mixture was treated in a manner similar to that described for **2P_{Zn}-CO₂H**, to give **4P_{Zn}-CO₂H** (0.13 g) as red powder in 58% yield. $R_f = 0.29$ ($\text{CH}_2\text{Cl}_2/\text{THF} = 100/5$ (v/v)). MS (MALDI-TOF, dithranol, reflector mode): m/z 3962.46 ($[\text{M} - \text{H}]^+$, calcd. for $\text{C}_{225}\text{H}_{166}\text{N}_{16}\text{O}_{38}\text{Zn}_4$: 3963.37). ^1H NMR (500 MHz, $\text{THF}-d_8$, 25 °C): δ (ppm) 10.26 (s, 8H, *meso*-H of P_{Zn}), 9.44–9.08 (m, 32H, pyrrole- β -H of P_{Zn}), 8.77 (d, $J = 8.0$ Hz, 8H, *o*-H of $\text{P}_{\text{Zn}}\text{C}_6\text{H}_4\text{CO}_2\text{Ar}$), 8.52 (d, $J = 8.0$ Hz, 8H, *m*-H of $\text{P}_{\text{Zn}}\text{C}_6\text{H}_4\text{CO}_2\text{Ar}$), 8.46 (d, $J = 2.0$ Hz, 4H, *o*-H of $\text{C}_6\text{H}_3\text{CO}_2\text{Ar}$), 8.18 (b, 2H, *o*-H of $\text{C}_6\text{H}_3\text{CO}_2\text{H}$), 8.12 (t, $J = 4.5$ Hz, 2H, *p*-H of $\text{C}_6\text{H}_3\text{CO}_2\text{Ar}$), 7.97 (b, 1H, *p*-H of $\text{C}_6\text{H}_3\text{CO}_2\text{H}$),

7.55 (d, $J = 3.0$ Hz, 8H, *o*-H of $\text{P}_{\text{Zn}}\text{C}_6\text{H}_3$), 7.15 (t, $J = 4.0$ Hz, 4H, *p*-H of $\text{P}_{\text{Zn}}\text{C}_6\text{H}_3$), 6.67 (d, $J = 2.5$ Hz, 16H, *o*-H of outer C_6H_3), 6.43 (t, $J = 4.5$ Hz, 8H, *p*-H of outer C_6H_3), 5.21 (s, 16H, ArCH_2OAr), 3.71 (s, 48H, ArOCH_3).

12P_{Zn}. To a THF solution (2 mL) of a mixture of **2P_{Zn}-CO₂H** (37.7 mg, 0.0196 mmol) and hexakis(4-hydroxyphenyl)benzene (1.24 mg, 1.97 μmol) was slowly added under Ar a CH_2Cl_2 solution (0.94 mL) of DPTS (2.87 mg, 0.00975 mmol). After 10 min, a CH_2Cl_2 solution (0.85 mL) of DCC (6.05 mg, 0.0293 mmol) was added to the above solution, and the mixture was stirred for 3 days at room temperature. The reaction mixture was treated in a manner similar to that described for **2P_{Zn}**, to give **12P_{Zn}** (21.1 mg) as red powder in 89% yield. $R_f = 0.70$ ($\text{CH}_2\text{Cl}_2/\text{THF} = 100/5$ (v/v)). MS (MALDI-TOF, dithranol, reflector mode): m/z 12060.85 ([M + H]⁺, calcd. for $\text{C}_{696}\text{H}_{510}\text{N}_{48}\text{O}_{108}\text{Zn}_{12}$: 12058.44). ¹H NMR (500 MHz, THF-*d*₈, 25 °C): δ (ppm) 10.08 (s, 24H, *meso*-H of P_{Zn}), 9.24–8.94 (m, 96H, pyrrole- β -H of P_{Zn}), 8.72 (d, $J = 8.0$ Hz, 24H, *o*-H of $\text{P}_{\text{Zn}}\text{C}_6\text{H}_4\text{CO}_2\text{Ar}$), 8.44 (d, $J = 2.0$ Hz, 12H, *o*-H of $(\text{ArCO}_2)_2\text{C}_6\text{H}_3\text{CO}_2\text{Ar}$), 8.39 (d, $J = 7.5$ Hz, 24H, *m*-H of $\text{P}_{\text{Zn}}\text{C}_6\text{H}_4\text{CO}_2\text{Ar}$), 8.06 (b, 6H, *p*-H of $(\text{ArCO}_2)_2\text{C}_6\text{H}_3\text{CO}_2\text{Ar}$), 7.49 (d, $J = 1.5$ Hz, 24H, *o*-H of $\text{P}_{\text{Zn}}\text{C}_6\text{H}_3$), 7.33–7.30 (m, 24H, *o*-H and *m*-H of $(\text{ArCO}_2\text{C}_6\text{H}_4)_6\text{C}_6$), 7.12 (b, 12H, *p*-H of $\text{P}_{\text{Zn}}\text{C}_6\text{H}_3$), 6.65 (m, 48H, *o*-H of outer C_6H_3), 6.41 (b, 24H, *p*-H of outer C_6H_3), 5.18 (s, 48H, ArCH_2OAr), 3.69 (s, 144H, ArOCH_3). UV-vis (CHCl_3 , 25 °C): 411.0, 542.6, 577.2 nm.

24P_{Zn}. To a THF solution (10 mL) of a mixture of **4P_{Zn}-CO₂H** (37.7 mg, 0.0196 mmol) and hexakis(4-hydroxyphenyl)benzene (6.9 mg, 1.97 μmol) was slowly added under Ar a CH_2Cl_2 solution (0.94 mL) of DPTS (2.86 mg, 0.00971 mmol). After 10 min, a CH_2Cl_2 solution (0.85 mL) of DCC (6.05 mg, 0.0293 mmol) was added to the above solution and the mixture was stirred for 4 days at room temperature. The reaction mixture was treated in a manner similar to that described for **2P_{Zn}**, to give **24P_{Zn}** (21.1 mg) as red powder in 89% yield. $R_f = 0.55$ ($\text{CH}_2\text{Cl}_2/\text{THF} = 100/5$ (v/v)). MS (MALDI-TOF, dithranol, linear mode): m/z 24407.27 (calcd. for $\text{C}_{1392}\text{H}_{1014}\text{N}_{96}\text{O}_{228}\text{Zn}_{24}$: 24302.81). ¹H NMR (500 MHz, THF-*d*₈, 25 °C): δ (ppm) 10.02 (s, 48H, *meso*-H of P_{Zn}), 9.18–8.90 (m, 192H, pyrrole- β -H of P_{Zn}), 8.59 (d, $J = 7.0$ Hz, 48H, *o*-H of $\text{P}_{\text{Zn}}\text{C}_6\text{H}_4\text{CO}_2\text{Ar}$), 8.41 (s, 24H, *o*-H of $(\text{P}_{\text{Zn}}\text{ArCO}_2)_2\text{C}_6\text{H}_3\text{CO}_2\text{Ar}$), 8.38 (s, 12H, *o*-H of $(\text{ArCO}_2)_2\text{C}_6\text{H}_3\text{CO}_2\text{Ar}$), 8.32 (d, $J = 7.0$ Hz, 48H, *m*-H of $\text{P}_{\text{Zn}}\text{C}_6\text{H}_4\text{CO}_2\text{Ar}$), 7.96–7.94 (m, 18H, *p*-H of $(\text{P}_{\text{Zn}}\text{ArCO}_2)_2\text{C}_6\text{H}_3\text{CO}_2\text{Ar}$ and *p*-H of $(\text{ArCO}_2)_2\text{C}_6\text{H}_3\text{CO}_2\text{Ar}$), 7.46 (s, 48H, *o*-H of $\text{P}_{\text{Zn}}\text{C}_6\text{H}_3$), 7.24 (b, 24H, *o*-H and *p*-H of $(\text{ArCO}_2\text{C}_6\text{H}_4)_6\text{C}_6$), 7.06 (s, 24H, *p*-H of $\text{P}_{\text{Zn}}\text{C}_6\text{H}_3$), 6.55 (d, $J = 2.0$ Hz, 96H, *o*-H of outer C_6H_3), 6.33 (s, 48H, *p*-H of outer C_6H_3), 5.07

(s, 96H, ArCH₂OAr), 3.60 (s, 288H, ArOCH₃). UV-vis (CHCl₃, 25 °C): 414.4, 543.2, 578.6 nm.

3P_{Zn}. To a THF solution (5 mL) of a mixture of **1P_{Zn}-CO₂H** (0.28 g, 0.31 mmol) and 2',2',2'-trichloroethyl 3,4,5-trihydroxybenzoate (27 mg, 0.088 mmol) was slowly added under Ar a CH₂Cl₂ solution (5 mL) of DPTS (46 mg, 0.17 mmol). After 10 min, a CH₂Cl₂ solution (5 mL) of DCC (100 mg, 0.48 mmol) was added to the above solution, and the mixture was stirred for 2 days at room temperature. The reaction mixture was treated in a manner similar to that described for **2P_{Zn}**, to give **3P_{Zn}** (0.25 g) as red powder in 96% yield. $R_f = 0.80$ (CH₂Cl₂/THF = 100/5 (v/v)). MS (MALDI-TOF, dithranol, reflector mode): m/z 2954.07 ([M + H]⁺). Anal. calcd. for C₁₆₂H₁₂₁Cl₃N₁₂O₂₆Zn₃ (2954.29): calcd. C 65.8, H 4.1, N 5.7, Cl 3.6, Zn 6.6; found C 64.2, H 4.4, N 5.3, Cl 3.3, Zn 6.0. ¹H NMR (500 MHz, CDCl₃, 25 °C): δ (ppm) 10.08 (s, 4H, *meso*-H of P_{Zn}), 9.61 (s, 2H, *meso*-H of P_{Zn}), 9.36 (d, *J* = 4.0 Hz, 4H, pyrrole-β-H of P_{Zn}), 9.19–9.18 (m, 6H, pyrrole-β-H of P_{Zn}), 9.16 (d, *J* = 4.0 Hz, 4H, pyrrole-β-H of P_{Zn}), 9.12–9.11 (m, 6H, pyrrole-β-H of P_{Zn}), 8.98 (d, *J* = 4.5 Hz, 2H, pyrrole-β-H of P_{Zn}), 8.88–8.85 (m, 6H, pyrrole-β-H of P_{Zn} and *o*-H of P_{Zn}C₆H₄CO₂Ar), 8.68 (d, *J* = 1.0 Hz, 2H, *o*-H of C₆H₂CO₂CH₂CCl₃), 8.61 (d, *J* = 8.0 Hz, 4H, *m*-H of P_{Zn}C₆H₄CO₂Ar), 8.57 (d, *J* = 7.0 Hz, 2H, *o*-H of P_{Zn}C₆H₄CO₂Ar), 8.54 (d, *J* = 4.5 Hz, 2H, *m*-H of P_{Zn}C₆H₄CO₂Ar), 7.61 (b, 4H, *o*-H of P_{Zn}C₆H₃), 7.56 (b, 2H, *o*-H of P_{Zn}C₆H₃), 7.21 (b, 2H, *p*-H of P_{Zn}C₆H₃), 7.19 (b, 1H, *p*-H of P_{Zn}C₆H₃), 6.73–6.72 (m, 12H, *o*-H of outer C₆H₃), 6.48 (b, 6H, *p*-H of outer C₆H₃), 5.36 (s, 2H, CO₂CH₂CCl₃), 5.27 (s, 8H, ArCH₂OAr), 5.25 (s, 4H, ArCH₂OAr), 3.76 (s, 24H, ArOCH₃), 3.75 (s, 12H, ArOCH₃). UV-vis (CHCl₃, 25 °C): 414.4, 544.2 nm.

3P_{Zn}-CO₂H. A THF/AcOH solution (5 mL/5 mL) of a mixture of **3P_{Zn}** (0.28 g, 0.096 mmol), and zinc powder (1.0 g, 15 mmol) was stirred for 12 h at 60 °C. The reaction mixture was treated in a manner similar to that described for **2P_{Zn}-CO₂H**, to give **3P_{Zn}-CO₂H** (0.19 g) as red powder in 72% yield. $R_f = 0.25$ (CH₂Cl₂/THF = 100/5 (v/v)). MS (MALDI-TOF, dithranol, reflector mode): m/z 2822.47 ([M - H]⁺, calcd. for C₁₆₀H₁₂₀N₁₂O₂₆Zn₃: 2822.9). ¹H NMR (500 MHz, CDCl₃, 25 °C): δ (ppm) 10.08 (s, 4H, *meso*-H of P_{Zn}), 9.59 (s, 2H, *meso*-H of P_{Zn}), 9.35 (d, *J* = 4.5 Hz, 4H, pyrrole-β-H of P_{Zn}), 9.18–9.15 (m, 12H, pyrrole-β-H of P_{Zn}), 9.11–9.09 (m, 6H, pyrrole-β-H of P_{Zn}), 8.96 (d, *J* = 4.0 Hz, 2H, pyrrole-β-H of P_{Zn}), 8.86–8.83 (m, 6H, pyrrole-β-H of P_{Zn} and *o*-H of P_{Zn}C₆H₄CO₂Ar), 8.59 (d, *J* = 8.0 Hz, 4H, *m*-H of P_{Zn}C₆H₄CO₂Ar), 8.57 (s, 2H, *o*-H of C₆H₂CO₂CH₂CCl₃), 8.55 (d, *J* = 8.0 Hz, 2H, *o*-H of

$P_{Zn}C_6H_4CO_2Ar$), 8.52 (d, $J = 4.5$ Hz, 2H, *m*-H of $P_{Zn}C_6H_4CO_2Ar$), 7.59 (d, $J = 3.0$ Hz, 4H, *o*-H of $P_{Zn}C_6H_3$), 7.53 (d, $J = 2.0$ Hz, 2H, *o*-H of $P_{Zn}C_6H_3$), 7.18 (t, $J = 4.0$ Hz, 2H, *p*-H of $P_{Zn}C_6H_3$), 7.17 (t, $J = 4.0$ Hz, 1H, *p*-H of $P_{Zn}C_6H_3$), 6.72 (d, $J = 2.5$ Hz, 8H, *o*-H of outer C_6H_3), 6.70 (d, $J = 2.5$ Hz, 4H, *o*-H of outer C_6H_3), 6.47–6.45 (m, 6H, *p*-H of outer C_6H_3), 5.25 (s, 8H, $ArCH_2OAr$), 5.23 (s, 4H, $ArCH_2OAr$), 3.75 (s, 24H, $ArOCH_3$), 3.74 (s, 12H, $ArOCH_3$).

6P_{Zn}. To a THF solution (3 mL) of a mixture of **3P_{Zn}-CO₂H** (0.13 g, 0.045 mmol) and 2',2',2'-trichloroethyl 3,5-dihydroxybenzoate (5.7 mg, 0.020 mmol) was slowly added under Ar a CH₂Cl₂ solution (2 mL) of DPTS (14 mg, 0.048 mmol). After 10 min, a CH₂Cl₂ solution (2 mL) of DCC (28 mg, 0.14 mmol) was added to the above solution, and the mixture was stirred for 2 days at room temperature. The reaction mixture was treated in a manner similar to that described for **2P_{Zn}**, to give **6P_{Zn}** (76 mg) as red powder in 65% yield. $R_f = 0.91$ (CH₂Cl₂/THF = 100/5 (v/v)). MS (MALDI-TOF, dithranol, reflector mode): m/z 5895.97 ([M + H]⁺, calcd. for C₃₂₉H₂₄₃Cl₃N₂₄O₅₄Zn₆: 5895.28). ¹H NMR (500 MHz, CDCl₃, 25 °C): δ (ppm) 10.08 (s, 8H, *meso*-H of P_{Zn}), 9.60 (s, 4H, *meso*-H of P_{Zn}), 9.34 (d, $J = 4.0$ Hz, 8H, pyrrole- β -H of P_{Zn}), 9.18–9.13 (m, 28H, pyrrole- β -H of P_{Zn}), 9.10 (d, $J = 4.0$ Hz, 4H, pyrrole- β -H of P_{Zn}), 8.99 (d, $J = 4.0$ Hz, 4H, pyrrole- β -H of P_{Zn}), 8.92–8.90 (m, 16H, pyrrole- β -H of P_{Zn} and *o*-H of $P_{Zn}C_6H_4CO_2Ar$ and *o*-H of (ArCO₂)₂C₆H₂CO₂Ar), 8.64 (d, $J = 8.0$ Hz, 8H, *m*-H of $P_{Zn}C_6H_4CO_2Ar$), 8.59 (d, $J = 8.0$ Hz, 4H, *o*-H of $P_{Zn}C_6H_4CO_2Ar$), 8.55 (d, $J = 4.5$ Hz, 4H, *m*-H of $P_{Zn}C_6H_4CO_2Ar$), 8.44 (d, $J = 1.5$ Hz, 2H, *o*-H of (ArCO₂)₂C₆H₃CO₂CH₂CCl₃), 8.26 (b, 1H, *p*-H of (ArCO₂)₂C₆H₃CO₂CH₂CCl₃), 7.58 (d, $J = 3.0$ Hz, 8H, *o*-H of P_{Zn}C₆H₃), 7.54 (d, $J = 2.0$ Hz, 4H, *o*-H of P_{Zn}C₆H₃), 7.18 (b, 4H, *p*-H of P_{Zn}C₆H₃), 7.17 (b, 2H, *p*-H of P_{Zn}C₆H₃), 6.72–6.71 (m, 24H, *o*-H of outer C_6H_3), 6.46 (b, 12H, *p*-H of outer C_6H_3), 5.35 (s, 2H, CO₂CH₂CCl₃), 5.26 (s, 16H, $ArCH_2OAr$), 5.24 (s, 8H, $ArCH_2OAr$), 3.75–3.74 (m, 72H, $ArOCH_3$). UV-vis (CHCl₃, 25 °C): 414.0, 543.2 nm.

6P_{Zn}-CO₂H. A THF/AcOH solution (3 mL/2 mL) of a mixture of **6P_{Zn}** (69 mg, 0.0117 mmol) and zinc powder (0.5 g, 7.6 mmol) was stirred for 12 h at 60 °C. The reaction mixture was treated in a manner similar to that described for **2P_{Zn}-CO₂H**, to give **6P_{Zn}-CO₂H** (41 mg) as red powder in 61% yield. $R_f = 0.14$ (CH₂Cl₂/THF = 100/5 (v/v)). MS (MALDI-TOF, dithranol, reflector mode): m/z 5762.33 ([M – H]⁺, calcd. for C₃₂₇H₂₄₂N₂₄O₅₄Zn₆: 5763.89). ¹H NMR (500 MHz, CDCl₃, 25 °C): δ (ppm) 10.08 (s, 8H, *meso*-H of P_{Zn}), 9.60 (s, 4H, *meso*-H of P_{Zn}), 9.34 (d, $J = 4.5$ Hz, 8H, pyrrole- β -H of P_{Zn}), 9.18–9.12 (m, 28H, pyrrole- β -H of P_{Zn}), 9.08 (d, $J = 4.0$ Hz, 4H, pyrrole- β -H of P_{Zn}), 8.97 (d,

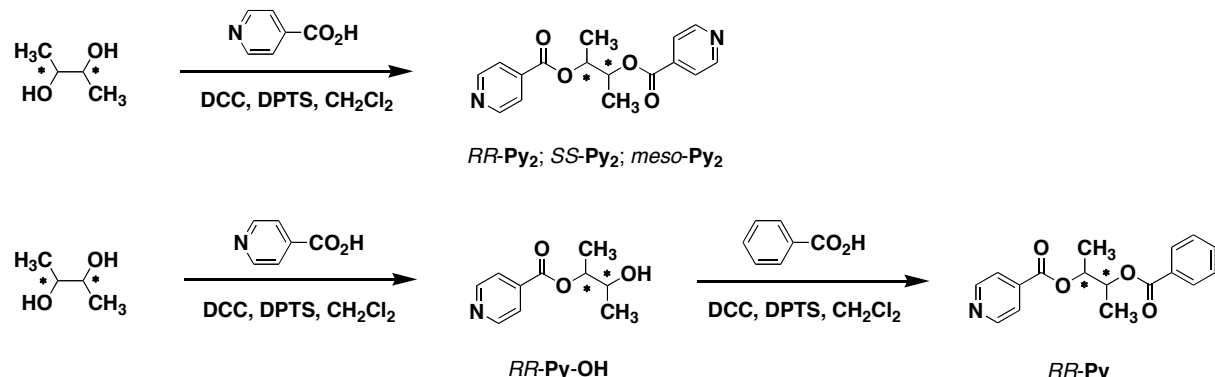
J = 4.0 Hz, 4H, pyrrole- β -H of P_{Zn}), 8.90–8.88 (m, 16H, pyrrole- β -H of P_{Zn} and *o*-H of P_{Zn}C₆H₄CO₂Ar and *o*-H of (ArCO₂)₂C₆H₂CO₂Ar), 8.63 (d, *J* = 8.0 Hz, 8H, *m*-H of P_{Zn}C₆H₄CO₂Ar), 8.58 (d, *J* = 8.5 Hz, 4H, *o*-H of P_{Zn}C₆H₄CO₂Ar), 8.54 (d, *J* = 4.0 Hz, 4H, *m*-H of P_{Zn}C₆H₄CO₂Ar), 8.32 (d, *J* = 2.0 Hz, 2H, *o*-H of (ArCO₂)₂C₆H₃CO₂CH₂CCl₃), 8.15 (m, 1H, *p*-H of (ArCO₂)₂C₆H₃CO₂CH₂CCl₃), 7.57 (d, *J* = 2.0 Hz, 8H, *o*-H of P_{Zn}C₆H₃), 7.52 (d, *J* = 1.5 Hz, 4H, *o*-H of P_{Zn}C₆H₃), 7.16 (t, *J* = 4.0 Hz, 4H, *p*-H of P_{Zn}C₆H₃), 7.15 (b, 2H, *p*-H of P_{Zn}C₆H₃), 6.71–6.69 (m, 24H, *o*-H of outer C₆H₃), 6.45 (t, *J* = 4.5 Hz, 12H, *p*-H of outer C₆H₃), 5.24 (s, 16H, ArCH₂OAr), 5.23 (s, 8H, ArCH₂OAr), 3.74 (d, 48H, ArOCH₃), 3.73 (s, 24H, ArOCH₃).

18P_{Zn}. To a THF solution (2 mL) of a mixture of **3P_{Zn}-CO₂H** (62 mg, 0.0221 mmol) and hexakis(4-hydroxyphenyl)benzene (1.52 mg, 0.00241 mmol) was slowly added under Ar a CH₂Cl₂ solution (2 mL) of DPTS (10 mg, 0.034 mmol). After 10 min, a CH₂Cl₂ solution (2 mL) of DCC (28.5 mg, 0.138 mmol) was added to the above solution, and the mixture was stirred for 6 days at room temperature. The reaction mixture was treated in a manner similar to that described for **2P_{Zn}**, to give **18P_{Zn}** (4.8 mg) as red powder in 11% yield. *R_f* = 0.86 (CH₂Cl₂/THF = 100/5 (v/v)). MS (MALDI-TOF, dithranol, linear mode): m/z 17479.00 (calcd. for C₁₀₀₂H₇₃₈N₇₂O₁₅₆Zn₁₈: 17459.99). ¹H NMR (500 MHz, THF-*d*₈, 25 °C): δ (ppm) 9.79 (s, 24H, *meso*-H of P_{Zn}), 9.42 (s, 12H, *meso*-H of P_{Zn}), 9.07–8.23 (m, 228H, pyrrole- β -H of P_{Zn} and P_{Zn}C₆H₄CO₂Ar and (P_{Zn}ArCO₂)₃C₆H₂CO₂Ar), 7.62–7.07 (m, 78H, P_{Zn}C₆H₃ and (ArCO₂C₆H₄)₆C₆), 6.67–6.30 (m, 108H, outer C₆H₃), 5.19–5.10 (s, 72H, ArCH₂OAr), 3.58 (m, 216H, ArOCH₃). UV-vis (CHCl₃, 25 °C): 413.0, 544.4, 578.8 nm.

36P_{Zn}. To a THF solution (0.8 mL) of a mixture of **6P_{Zn}-CO₂H** (32.1 mg, 5.56 μmol) and hexakis(4-hydroxyphenyl)benzene (0.356 mg, 0.565 μmol) was slowly added under Ar a CH₂Cl₂ solution (1 mL) of DPTS (9.8 mg, 0.0333 mmol). After 10 min, a CH₂Cl₂ solution (1 mL) of DCC (23 mg, 0.111 mmol) was added to the above solution, and the mixture was stirred for 7 days at room temperature. The reaction mixture was treated in a manner similar to that described for **2P_{Zn}**, to give **36P_{Zn}** (7.8 mg) as red powder in 39% yield. *R_f* = 0.84 (CH₂Cl₂/THF = 100/5 (v/v)). MS (MALDI-TOF, dithranol, linear mode): m/z 35314.08 (calcd. for C₂₀₀₄H₁₄₇₀N₁₄₄O₃₂₄Zn₃₆: 35105.93). ¹H NMR (500 MHz, THF-*d*₈, 25 °C): δ (ppm) 9.79 (b, 72H, *meso*-H of P_{Zn}), 8.94–8.07 (m, 474H, pyrrole- β -H of P_{Zn}, P_{Zn}C₆H₄CO₂Ar, (P_{Zn}ArCO₂)₃C₆H₂CO₂Ar, and (ArCO₂)₂C₆H₃CO₂Ar), 7.39–7.03 (m, 132H, P_{Zn}C₆H₃ and (ArCO₂C₆H₄)₆C₆), 6.70–6.25 (m, 216H, outer C₆H₃), 5.11–4.98 (b, 144H, ArCH₂OAr), 3.58 (b,

432H, ArOCH₃). UV-vis (CHCl₃, 25 °C): 414.2, 544.4, 579.4 nm.

(2) Synthesis of guests



Scheme S3. Synthesis of guests

***RR-Py*₂.** To a CH₂Cl₂ solution (15 mL) of a mixture of isonicotinic acid (347.5 mg, 2.82 mmol), (2*R*,3*R*)(-)-2,3-butandiol (100 mg, 1.11 mmol), and DPTS (335.7 mg, 1.14 mmol) was added under Ar a CH₂Cl₂ solution (15 mL) of DCC (1.44 g, 6.98 mmol), and the mixture was stirred for 2 days at room temperature. The insoluble fraction was filter off, and the filtrate was concentrated and chromatographed on silica gel with CH₂Cl₂/MeOH (100/5 (v/v)) as an eluent, to give *RR-Py*₂ (317 mg) in 95% yield. *R*_f = 0.28 (CH₂Cl₂/MeOH = 100/5). MS (MALDI-TOF, CHCA, reflector mode): m/z 301.06 ([M + H]⁺, calcd. for C₁₆H₁₆N₂O₄: 300.31). ¹H NMR (500 MHz, CDCl₃, 25 °C): δ (ppm) 8.75 (d, *J* = 5.5 Hz, 4H, *o*-*H* of pyridyl), 7.82 (d, *J* = 5.0 Hz, 4H, *m*-*H* of pyridyl), 5.38 (m, 2H, CHCH₃), 1.43 (d, *J* = 6.0 Hz, 6H, CHCH₃).

***SS-Py*₂.** *SS-Py*₂ was synthesized in 90% yield from (2*S*,3*S*)(+)-2,3-butandiol in a manner similar to that described for *RR-Py*₂. *R*_f = 0.28 (CH₂Cl₂/MeOH = 100/5 (v/v)). MS (MALDI-TOF, CHCA, reflector mode): m/z 301.05 ([M + H]⁺, calcd. for C₁₆H₁₆N₂O₄: 300.31). ¹H NMR (500 MHz, CDCl₃, 25 °C): δ (ppm) 8.69 (d, *J* = 5.5 Hz, 4H, *o*-*H* of pyridyl), 7.73 (d, *J* = 6.0 Hz, 4H, *m*-*H* of pyridyl), 5.33 (m, 2H, CHCH₃), 1.38 (d, *J* = 6.0 Hz, 6H, CHCH₃).

***meso-Py*₂.** *meso-Py*₂ was synthesized from *meso*-2,3-butandiol in 96% in a manner similar to that described for *RR-Py*₂. *R*_f = 0.28 (CH₂Cl₂/MeOH = 100/5 (v/v)). MS (MALDI-TOF, CHCA, reflector mode): m/z 301.07 ([M + H]⁺, calcd. for C₁₆H₁₆N₂O₄: 300.31). ¹H NMR

(500 MHz, CDCl₃, 25 °C): δ (ppm) 8.75 (d, *J* = 5.5 Hz, 4H, *o*-H of pyridyl), 7.74 (d, *J* = 6.0 Hz, 4H, *m*-H of pyridyl), 5.41 (m, 2H, CHCH₃), 1.44 (d, *J* = 6.0 Hz, 6H, CHCH₃).

RR-Py-OH. To a CH₂Cl₂ solution (50 mL) of a mixture of isonicotinic acid (1.70 g, 13.8 mmol), (2*R*,3*R*)-(-)-2,3-butandiol (0.84 mL, 9.25 mmol), and DPTS (0.72 g, 2.45 mmol) was added slowly a CH₂Cl₂ solution (10 mL) of DCC (3.87 g, 18.7 mmol), and the mixture was stirred for 1 day at room temperature. The insoluble fraction was filtered off, and the filtrate was concentrated and chromatographed on silica gel with CH₂Cl₂/MeOH (100/5 (v/v)) as an eluent, to give **RR-Py-OH** (1.03 g) in 57% yield. *R*_f = 0.11 (CH₂Cl₂/MeOH = 100/5 (v/v)). MS (MALDI-TOF, CHCA, reflector mode): m/z 196.06 ([M + H]⁺, calcd. for C₁₀H₁₃NO₃: 195.22). ¹H NMR (500 MHz, CDCl₃, 25 °C): δ (ppm) 8.77 (d, *J* = 6.5 Hz, 2H, *o*-H of pyridyl), 7.88 (d, *J* = 5.0 Hz, 2H, *m*-H of pyridyl), 5.05 (m, 1H, PyCO₂CHCH₃), 3.90 (m, 1H, HOCHCH₃), 2.07 (b, 1H, OH), 1.35 (d, *J* = 6.0 Hz, 3H, PyCO₂CHCH₃), 1.25 (d, *J* = 6.5 Hz, 3H, HOCHCH₃).

RR-Py. To a CH₂Cl₂ solution (30 mL) of a mixture of **RR-Py-OH** (1.03 g, 5.28 mmol), benzoic acid (0.97 g, 7.91 mmol), and DPTS (0.31 g, 1.06 mmol) was added slowly a CH₂Cl₂ solution (20 mL) of DCC (1.63 g, 7.91 mmol), and the mixture was stirred for 1 day at room temperature. The insoluble fraction was filtered off, and the filtrate was concentrated and chromatographed on silica gel with CH₂Cl₂/MeOH (100/5 (v/v)) as an eluent, to give **RR-Py** (0.99 g) in 63% yield. *R*_f = 0.51 (CH₂Cl₂/MeOH = 100/5 (v/v)). MS (MALDI-TOF, dithranol, reflector mode): m/z 299.99 ([M + H]⁺, calcd. for C₁₇H₁₇NO₄: 299.32). ¹H NMR (500 MHz, CDCl₃, 25 °C): δ (ppm) 8.73 (d, *J* = 6.0 Hz, 2H, *o*-H of pyridyl), 7.99 (m, 2H, *o*-H of C₆H₅), 7.84 (d, *J* = 6.5 Hz, 2H, *m*-H of pyridyl), 7.52 (m, 1H, *p*-H of C₆H₅), 7.39 (m, 2H, *m*-H of C₆H₅), 5.36 (m, 2H, CHCH₃), 1.42 (m, 6H, CHCH₃).

4. Mass spectra

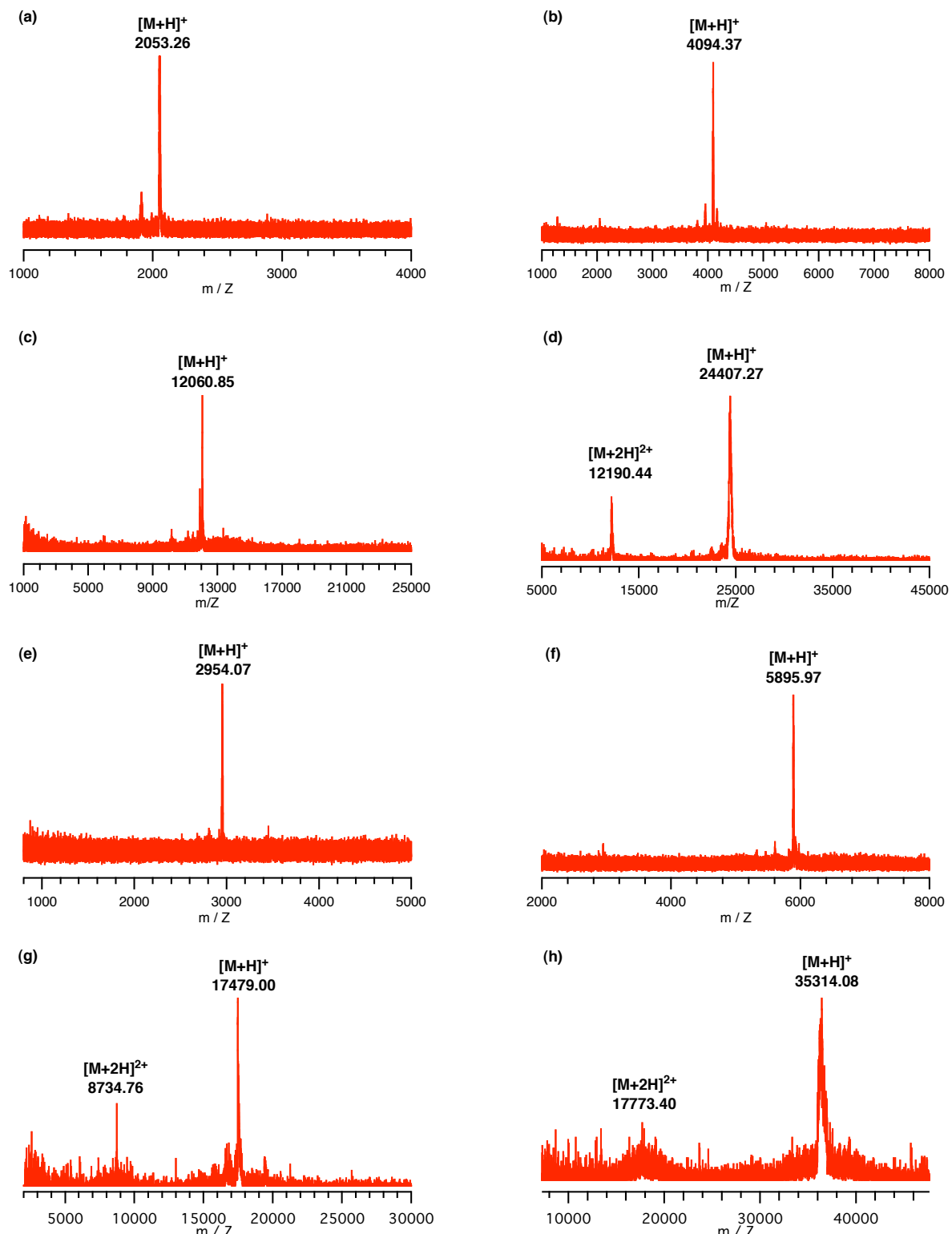


Figure S1. MALDI-TOF-MS spectra of (a) **2P_{Zn}** (reflector mode), (b) **4P_{Zn}** (reflector mode), (c) **12P_{Zn}** (reflector mode), (d) **24P_{Zn}** (linear mode), (e) **3P_{Zn}** (reflector mode), (f) **6P_{Zn}** (reflector mode), (g) **18P_{Zn}** (linear mode), and (h) **36P_{Zn}** (linear mode), using dithranol as a matrix.

5. Electronic absorption spectra of 2P_{Zn} , 3P_{Zn} , 4P_{Zn} , 6P_{Zn} , 12P_{Zn} , 18P_{Zn} , 24P_{Zn} , and 36P_{Zn}

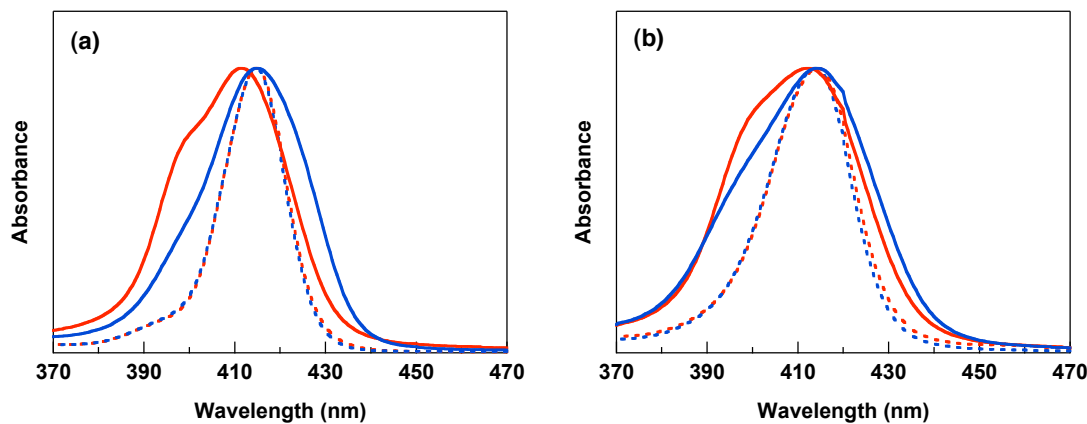


Figure S2. Normalized absorption spectra of (a) 2P_{Zn} (red broken curve), 4P_{Zn} (blue broken curve), 12P_{Zn} (red solid curve), and 24P_{Zn} (blue solid curve), and (b) 3P_{Zn} (red broken curve), 6P_{Zn} (blue broken curve), 18P_{Zn} (red solid curve), and 36P_{Zn} (blue solid curve) in CHCl_3 at 25 °C.

6. CD spectra of guests

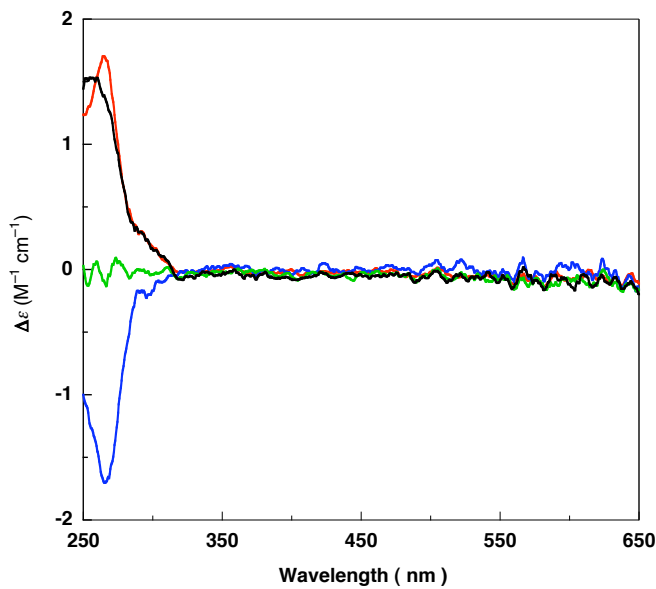


Figure S3. CD spectra of **RR-Py₂** (red curve), **SS-Py₂** (blue curve), **meso-Py₂** (green curve), and **RR-Py** (black curve) in CHCl_3 at 25 °C.

7. UV-vis and CD spectral titration of **24P_{Zn}** with **RR-Py₂**

Typical procedures for spectroscopic titration and evaluation of association constants K_{assoc} : Aliquots of a CHCl₃ solution of **RR-Py₂** (3.68×10^{-2} M) were added to a CHCl₃ solution of **24P_{Zn}** (0.21 μ M) ($[\text{RR-Py}_2]/[\text{24P}_{\text{Zn}}] = 0\text{--}2000$), and the mixture was subjected to UV-vis and CD spectroscopies at 25 °C. Each spectrum was corrected with a dilution factor and background subtraction. The difference in absorbance (ΔA) of **24P_{Zn}** in the presence (A ; $A_\infty = A$ at infinite [RR-Py₂]) and absence (A_0) of **RR-Py₂** was measured at 400, 414.8, 500, and 535 nm, and the data were plotted against [RR-Py₂]. The UV-vis spectral change upon titration exhibited isosbestic points, indicating that each zinc porphyrin unit in **24P_{Zn}** binds independently with a pyridyl unit. Thus, association constant K_{assoc} was evaluated by non-linear curve fitting using the equation: $\Delta A = \Delta A_\infty ((1 + K_{\text{assoc}}[\text{Py}] + K_{\text{assoc}}[\text{P}_{\text{Zn}}]_0) - ((1 + K_{\text{assoc}}[\text{Py}] + K_{\text{assoc}}[\text{P}_{\text{Zn}}]_0)^2 - 4 K_{\text{assoc}}^2 [\text{P}_{\text{Zn}}]_0 [\text{Py}]^{0.5}) / (2 K_{\text{assoc}} [\text{P}_{\text{Zn}}]_0)$, where $\Delta A = A - A_0$, $\Delta A_\infty = A_\infty - A_0$, $[\text{Py}] = 2[\text{RR-Py}_2]$, $[\text{P}_{\text{Zn}}] = 24[\text{24P}_{\text{Zn}}]$.⁶

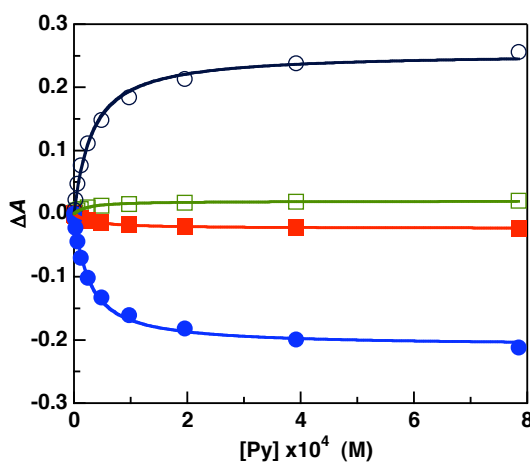
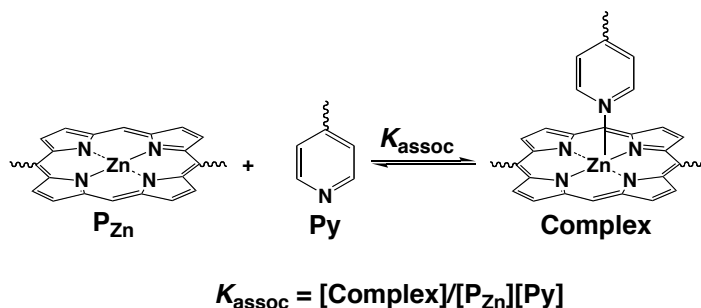


Figure S4. UV-vis absorbance data of **24P_{Zn}** (0.21 μ M) upon titration with **RR-Py₂**, monitored at 400 (blue filled circles), 414.8 (black open circles), 535 (red filled squares), and 550 nm (green open squares) in CHCl₃ at 25 °C, and their curve-fitting profiles (solid curves).

8. Association constants of zinc porphyrin-appended dendrons and dendrimers with chiral guests

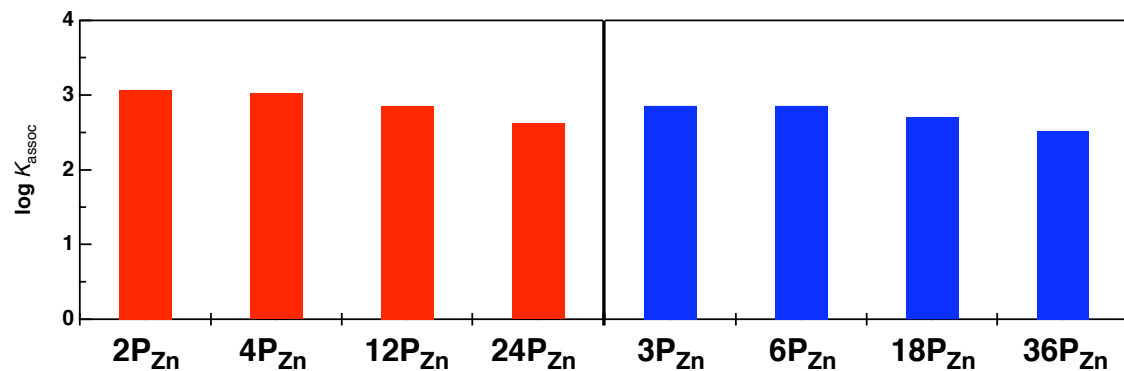


Figure S5. Association constants ($\log K_{\text{assoc}}$) of $2\mathbf{P}_{\text{Zn}}$, $3\mathbf{P}_{\text{Zn}}$, $4\mathbf{P}_{\text{Zn}}$, $6\mathbf{P}_{\text{Zn}}$, $12\mathbf{P}_{\text{Zn}}$, $18\mathbf{P}_{\text{Zn}}$, $24\mathbf{P}_{\text{Zn}}$, and $36\mathbf{P}_{\text{Zn}}$ with *RR*-Py in CHCl_3 at 25 °C.

9. Spectroscopic titration of **24P_{Zn}** with **RR-Py₂**, **SS-Py₂**, **meso-Py₂**, and **RR-Py**

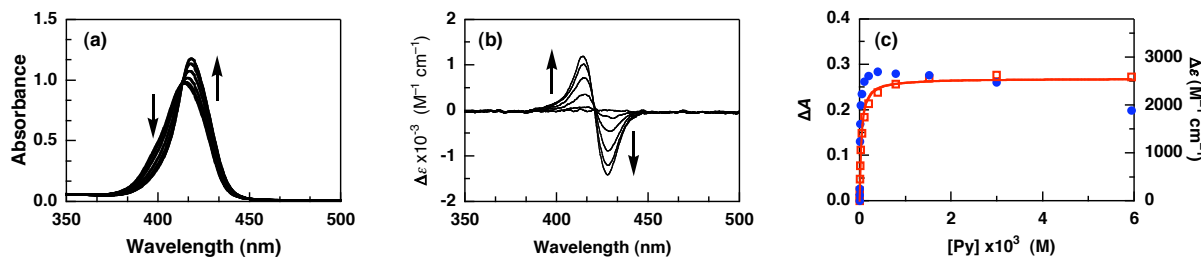


Figure S6. (a) UV–vis and (b) CD spectral changes of **24P_{Zn}** ($0.21 \mu\text{M}$) upon titration with **RR-Py₂** ($[\text{RR-Py}_2]/[\text{24P}_{\text{Zn}}] = 0, 6, 29, 116, 473, \text{ and } 1903$) in CHCl_3 at 25°C , and (c) UV–vis absorbance data monitored at 418.4 nm (red open squares) and their curve–fitting profile (red solid curve), and CD amplitudes (blue close circles).

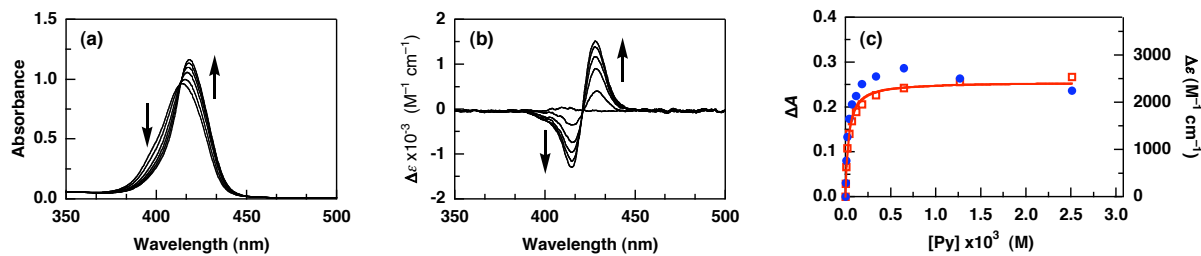


Figure S7. (a) UV–vis and (b) CD spectral changes of **24P_{Zn}** ($0.19 \mu\text{M}$) upon titration with **SS-Py₂** ($[\text{SS-Py}_2]/[\text{24P}_{\text{Zn}}] = 0, 24, 106, 311, 884, \text{ and } 3342$) in CHCl_3 at 25°C , and (c) UV–vis absorbance data monitored at 418.4 nm (red open squares) and their curve–fitting profile (red solid curve), and CD amplitudes (blue close circles).

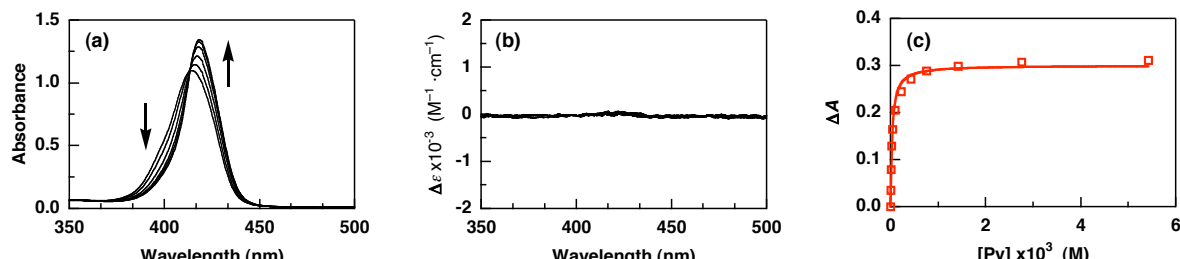


Figure S8. (a) UV–vis and (b) CD spectral changes of **24P_{Zn}** ($0.22 \mu\text{M}$) upon titration with **meso-Py₂** ($[\text{meso-Py}_2]/[\text{24P}_{\text{Zn}}] = 0, 22, 89, 512, 1726, \text{ and } 6280$) in CHCl_3 at 25°C , and (c) UV–vis absorbance data monitored at 418.4 nm (red open squares) and their curve–fitting profile (red solid curve).

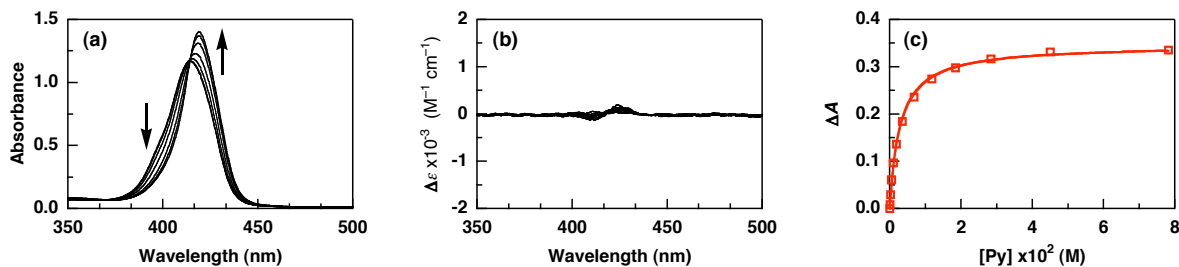


Figure S9. (a) UV-vis and (b) CD spectral changes of **24P_{Zn}** (0.23 μ M) upon titration with **RR-Py** ($[RR\text{-Py}]/[24P_{Zn}] = 0, 218, 2185, 7948, 29417, 79512$, and 340000) in CHCl₃ at 25 °C, and (c) UV-vis absorbance data monitored at 419.4 nm (red open squares) and their curve-fitting profile (red solid curve).

10. Spectroscopic titration of $2\mathbf{P}_{\mathbf{Zn}}$, $3\mathbf{P}_{\mathbf{Zn}}$, $4\mathbf{P}_{\mathbf{Zn}}$, $6\mathbf{P}_{\mathbf{Zn}}$, $12\mathbf{P}_{\mathbf{Zn}}$, $18\mathbf{P}_{\mathbf{Zn}}$, and $36\mathbf{P}_{\mathbf{Zn}}$ with $RR\text{-Py}_2$ and $RR\text{-Py}$

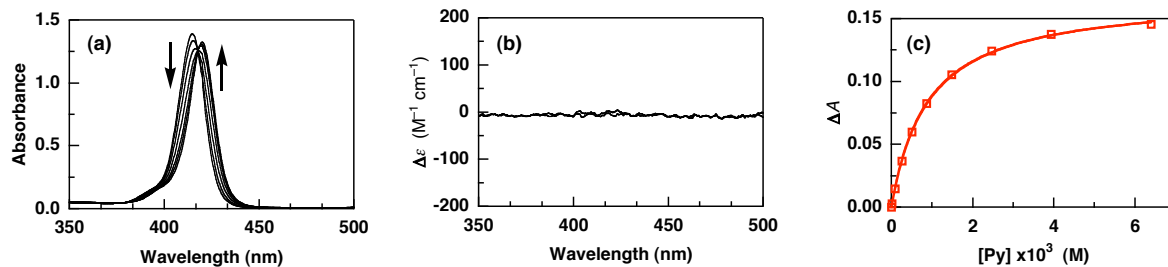


Figure S10. (a) UV–vis and (b) CD spectral changes of $2\mathbf{P}_{\mathbf{Zn}}$ ($1.03 \mu\text{M}$) upon titration with $RR\text{-Py}_2$ ($[RR\text{-Py}_2]/[2\mathbf{P}_{\mathbf{Zn}}] = 0, 41, 125, 244, 723$, and 3113) in CHCl_3 at 25°C , and (c) UV–vis absorbance data monitored at 420.0 nm (red open squares) and their curve–fitting profile (red solid curve).

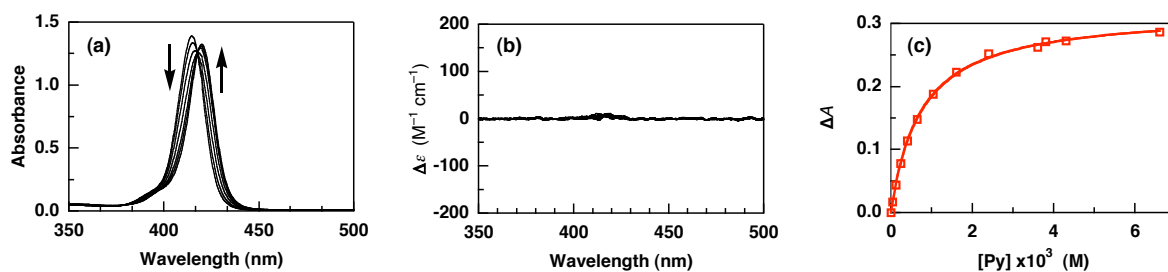


Figure S11. (a) UV–vis and (b) CD spectral changes of $2\mathbf{P}_{\mathbf{Zn}}$ ($1.88 \mu\text{M}$) upon titration with $RR\text{-Py}$ ($[RR\text{-Py}]/[2\mathbf{P}_{\mathbf{Zn}}] = 0, 63, 212, 553, 1276, 2020$, and 3507) in CHCl_3 at 25°C , and (c) UV–vis absorbance data monitored at 420.0 nm (red open squares) and their curve–fitting profile (red solid curve).

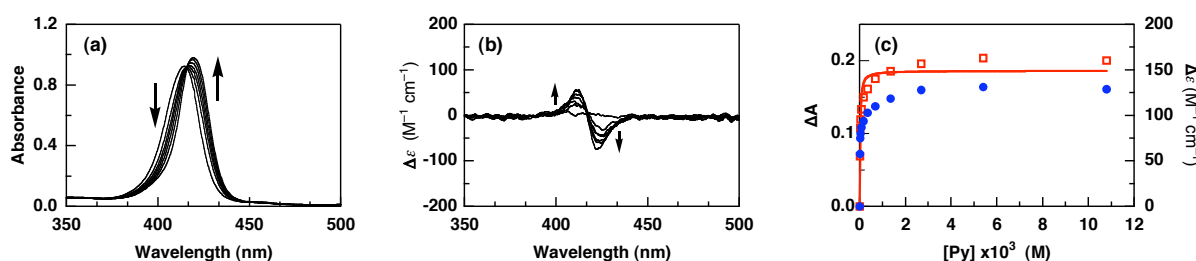


Figure S12. (a) UV–vis and (b) CD spectral changes of $3\mathbf{P}_{\mathbf{Zn}}$ ($1.39 \mu\text{M}$) upon titration with $RR\text{-Py}_2$ ($[RR\text{-Py}_2]/[3\mathbf{P}_{\mathbf{Zn}}] = 0, 2, 7, 24, 121, 486$, and 3890) in CHCl_3 at 25°C , and (c) UV–vis absorbance data monitored at 419.4 nm (red open squares) and their curve–fitting profile (red solid curve), and CD amplitudes (blue solid circles).

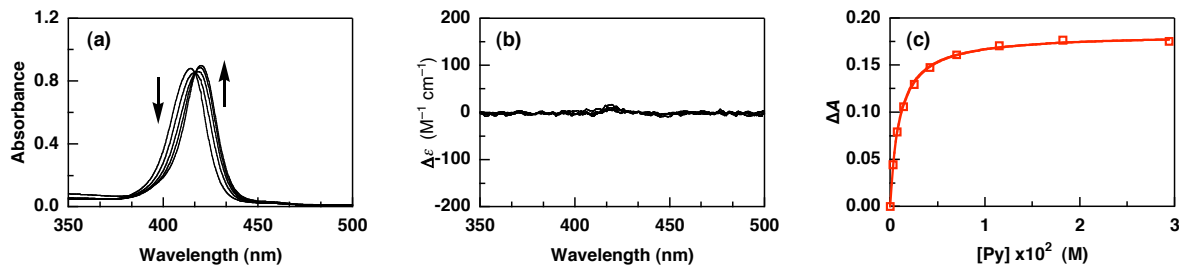


Figure S13. (a) UV-vis and (b) CD spectral changes of $3P_{Zn}$ ($1.28 \mu M$) upon titration with $RR\text{-Py}$ ($[RR\text{-Py}]/[3P_{Zn}] = 0, 569, 1971, 5474$, and 22991) in $CHCl_3$ at $25^\circ C$, and (c) UV-vis absorbance data monitored at 420.0 nm (red open squares) and their curve-fitting profile (red solid curve).

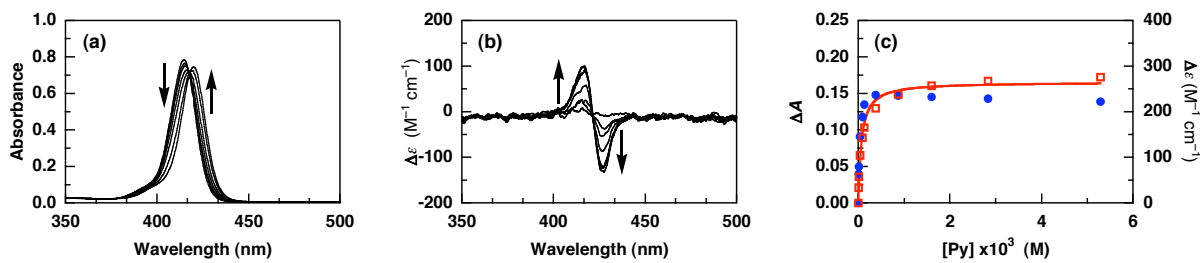


Figure S14. (a) UV-vis and (b) CD spectral changes of $4P_{Zn}$ ($0.61 \mu M$) upon titration with $RR\text{-Py}_2$ ($[RR\text{-Py}_2]/[4P_{Zn}] = 0, 4.91, 9.80, 29.5, 105.4, 708.7$, and 4328) in $CHCl_3$ at $25^\circ C$, and (c) UV-vis absorbance data monitored at 420.0 nm (red open squares) and their curve-fitting profile (red solid curve), and CD amplitudes (blue close circles).

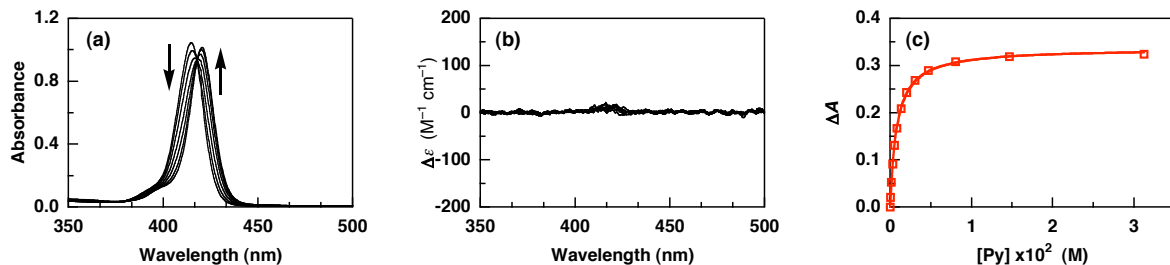


Figure S15. (a) UV-vis and (b) CD spectral changes of $4P_{Zn}$ ($0.85 \mu M$) upon titration with $RR\text{-Py}$ ($[RR\text{-Py}]/[4P_{Zn}] = 0, 178.3, 594.5, 1546, 3567, 9407$, and 36663) in $CHCl_3$ at $25^\circ C$, and (c) UV-vis absorbance data monitored at 420.4 nm (red open squares) and their curve-fitting profile (red solid curve).

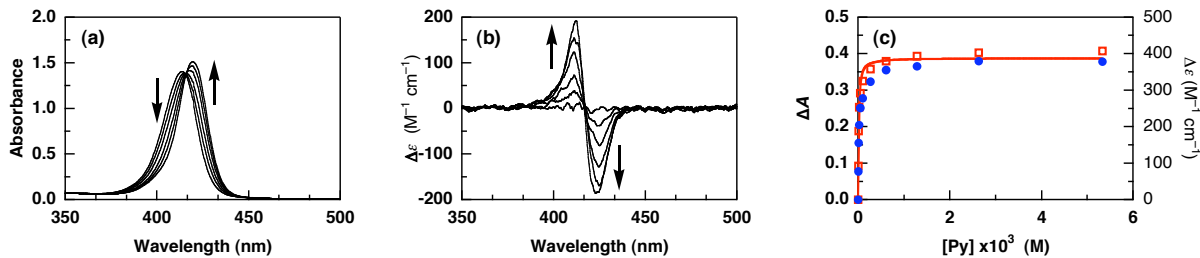


Figure S16. (a) UV–vis and (b) CD spectral changes of **6P_{Zn}** ($0.95 \mu\text{M}$) upon titration with **RR-Py₂** ($[\text{RR-Py}_2]/[\text{6P}_{\text{Zn}}] = 0, 1.77, 5.32, 24.82, 141.82, \text{ and } 2801$) in CHCl_3 at 25°C , and (c) UV–vis absorbance data monitored at 419.6 nm (red open squares) and their curve–fitting profile (red solid curve), and CD amplitudes (blue close circles).

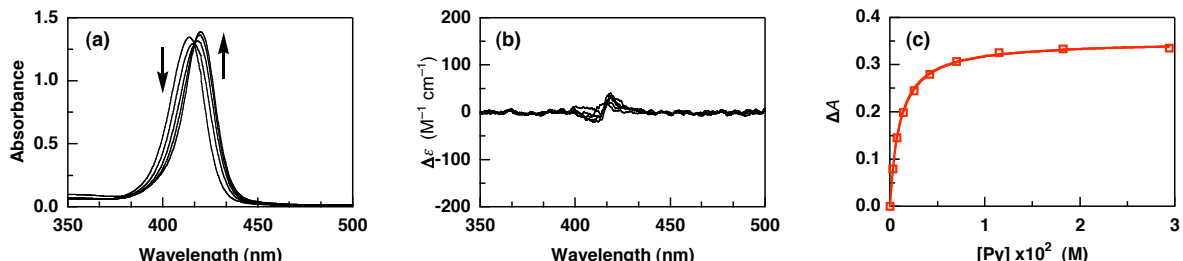


Figure S17. (a) UV–vis and (b) CD spectral changes of **6P_{Zn}** ($0.93 \mu\text{M}$) upon titration with **RR-Py** ($[\text{RR-Py}]/[\text{6P}_{\text{Zn}}] = 0, 781, 2703, 7508, \text{ and } 31532$) in CHCl_3 at 25°C , and (c) UV–vis absorbance data monitored at 420.0 nm (red open squares) and their curve–fitting profile (red solid curve).

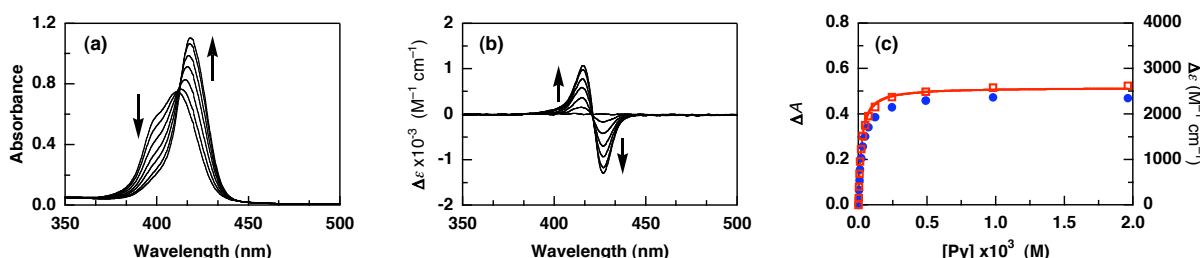


Figure S18. (a) UV–vis and (b) CD spectral changes of **12P_{Zn}** ($0.40 \mu\text{M}$) upon titration with **RR-Py₂** ($[\text{RR-Py}_2]/[\text{12P}_{\text{Zn}}] = 0, 4, 15, 39, 89, 303, \text{ and } 1218$) in CHCl_3 at 25°C , and (c) UV–vis absorbance data monitored at 418.4 nm (red open squares) and their curve–fitting profile (red solid curve), and CD amplitudes (blue close circles).

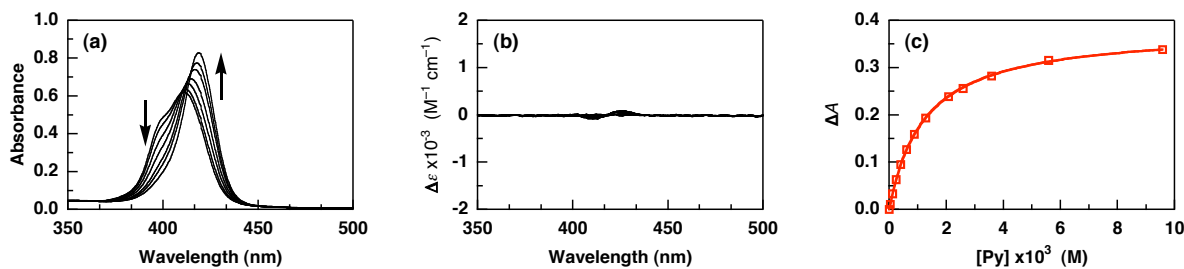


Figure S19. (a) UV–vis and (b) CD spectral changes of **12P_{Zn}** ($0.34 \mu\text{M}$) upon titration with **RR-Py** ($[\text{RR-Py}]/[\text{12P}_{\text{Zn}}] = 0, 353, 1176, 2587, 7582, 10516, \text{ and } 28120$) in CHCl_3 at 25°C , and (c) UV–vis absorbance data monitored at 418.4nm (red open squares) and their curve–fitting profile (red solid curve).

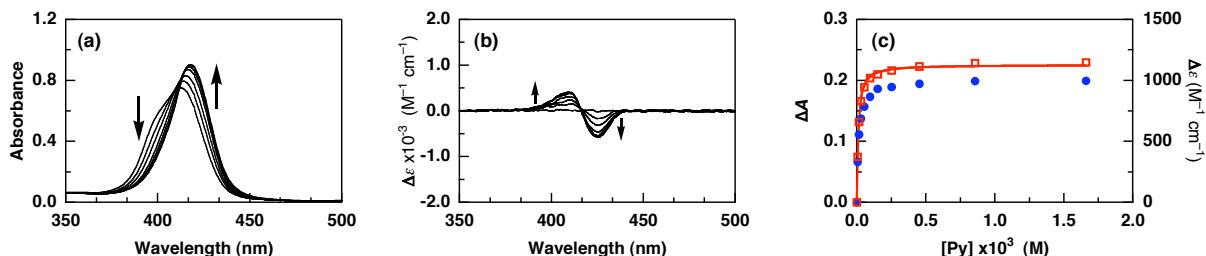


Figure S20 (a) UV–vis and (b) CD spectral changes of **18P_{Zn}** ($0.30 \mu\text{M}$) upon titration with **RR-Py₂** ($[\text{RR-Py}_2]/[\text{18P}_{\text{Zn}}] = 0, 8, 25, 92, 251, 754, \text{ and } 2766$) in CHCl_3 at 25°C , and (c) UV–vis absorbance data monitored at 418.0 nm (red open squares) and their curve–fitting profile (red solid curve), and CD amplitudes (blue close circles).

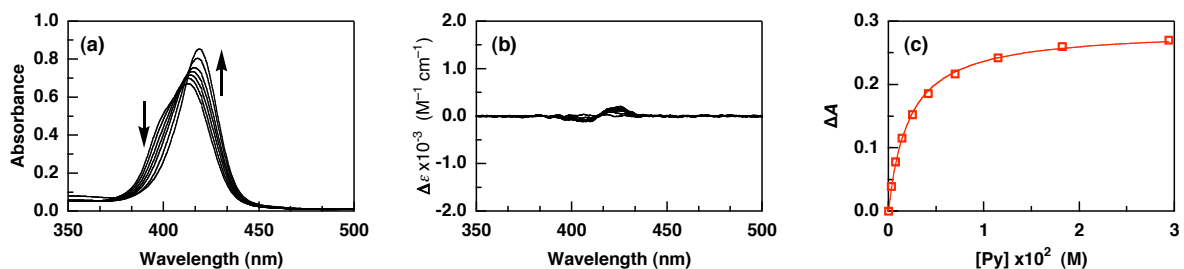


Figure S21. (a) UV–vis and (b) CD spectral changes of **18P_{Zn}** ($0.23 \mu\text{M}$) upon titration with **RR-Py** ($[\text{RR-Py}]/[\text{18P}_{\text{Zn}}] = 0, 1232, 3203, 6161, 11089, 30803, \text{ and } 129376$) in CHCl_3 at 25°C , and (c) UV–vis absorbance data monitored at 419.0 nm (red open squares) and their curve–fitting profile (blue solid curve).

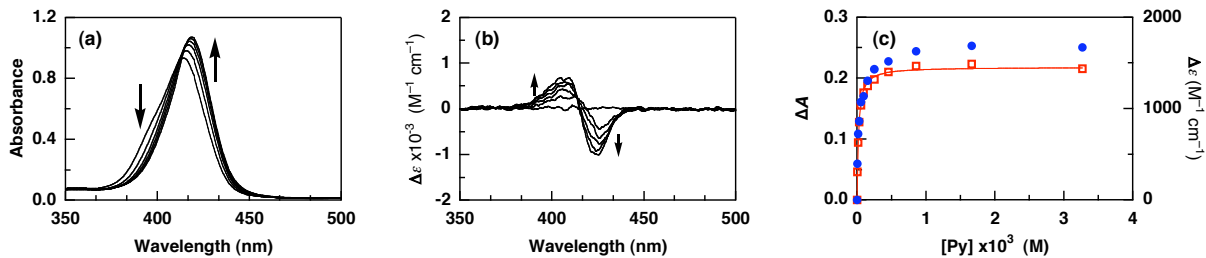


Figure S22. (a) UV-vis and (b) CD spectral changes of **36P_{Zn}** ($0.15 \mu\text{M}$) upon titration with **RR-Py₂** ($[\text{RR-Py}_2]/[\text{36P}_{\text{Zn}}] = 0, 50, 183, 501, 1505, \text{ and } 5519$) in CHCl_3 at 25°C , and (c) UV-vis absorbance data monitored at 418.8 nm (red open squares) and their curve-fitting profile (red solid curve), and CD amplitudes (blue close circles).

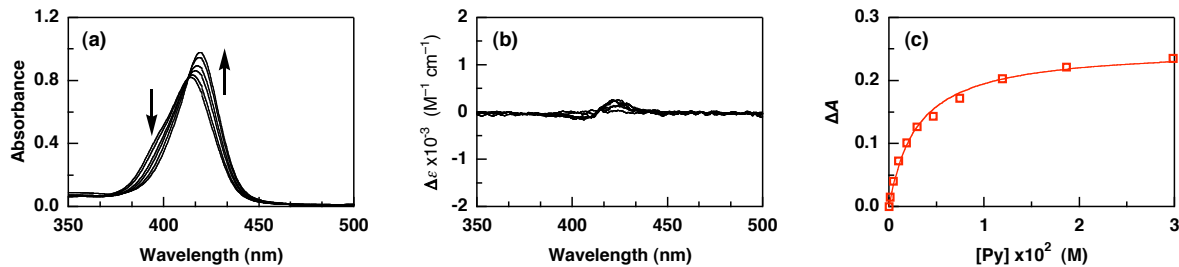


Figure S23. (a) UV-vis and (b) CD spectral changes of **36P_{Zn}** ($0.136 \mu\text{M}$) upon titration with **RR-Py** ($[\text{RR-Py}]/[\text{36P}_{\text{Zn}}] = 0, 3292, 13580, 34157, 87654, \text{ and } 219343$) in CHCl_3 at 25°C , and (c) UV-vis absorbance data monitored at 419.0 nm (red open squares) and their curve-fitting profile (red solid curve).

11. References

- (1) Littler, B. J.; Miller, M.A.; Huang, C-H.; Wagner, R. W.; O'Shea, D. F.; Boyle, P. D.; Lindsey, J. S. *J. Org. Chem.* **1999**, *64*, 1391–1396.
- (2) Horenstein, B. A.; Nakanishi, K. *J. Am. Chem. Soc.* **1989**, *111*, 6242–6246.
- (3) Hawker, C. J.; Fréchet, J. M. J. *J. Am. Chem. Soc.* **1992**, *114*, 8405–8413.
- (4) Kobayashi, K.; Shiraasaka, T., Sato, A.; Horn, E.; Fukukawa, N. *Angew. Chem. Int. Ed.* **1999**, *38*, 3483–3486.
- (5) Moore, J. S.; Stupp, S. I. *Macromolecules* **1990**, *23*, 65–70.
- (6) Connors, K.A. *Binding Constants*, Wiley, New York, **1987**.